CHALMERS
UNIVERSITY OF TECHNOLOGY

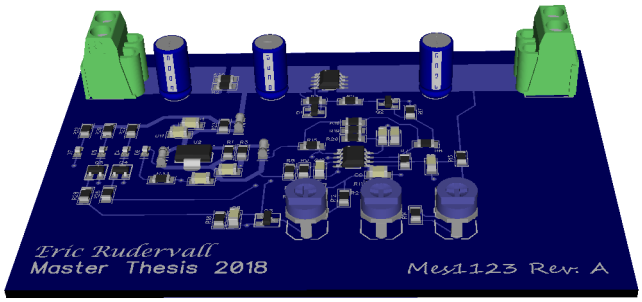

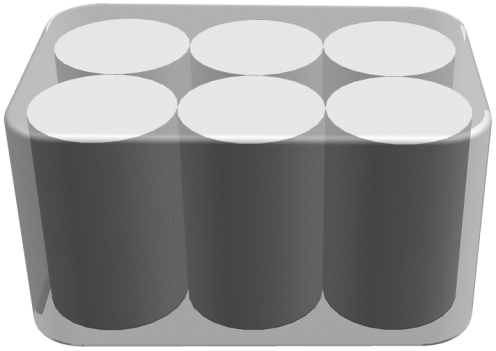

Supercapacitors as replacement for lead-acid batteries

A proof of concept solution for the future of power supply in automotive vehicles.

Master's thesis in Electric Power Engineering

ERIC RUDERVALL

Department of Electrical Engineering
CHALMERS UNIVERSITY OF TECHNOLOGY
Gothenburg, Sweden 2017

Master's thesis 2018: EENX30

Supercapacitors as replacement for lead-acid batteries

A proof of concept solution for the future of power supply in automotive vehicles.

ERIC RUDERVALL

CHALMERS
UNIVERSITY OF TECHNOLOGY

Department of Electrical Engineering
Division of Electric Power Engineering
Chalmers University of Technology
Gothenburg, Sweden 2018

Supercapacitors as replacement for lead-acid batteries
A proof of concept solution for the future of power supply in automotive vehicles.
ERIC RUDERVALL

© ERIC RUDERVALL, 2018.

Supervisor: Björn Lövhammer, Systems Manager Power Supply, CEVT AB
Supervisor: Alexander Engström, System Engineer Power Supply, CEVT AB
Examiner: Torbjörn Thiringer, Department of Electrical Engineering

Master's Thesis 2018: EENX30
Department of Electrical Engineering
Division of Electric Power Engineering
Chalmers University of Technology
SE-412 96 Gothenburg
Telephone +46 31 772 1000

Cover: Custom PCB designed for this project along with a hypothetical design of a supercapacitor module.

Typeset in LaTeX
Gothenburg, Sweden 2018

Super Capacitors as replacement for lead-acid batteries
A proof of concept solution for the future of power supply in automotive vehicles.
ERIC RUDERVALL
Department of Electrical Engineering
Chalmers University of Technology

Abstract

The automotive industry is a fast-paced, continuously progressing industry in terms of technological advancement. A component in the fossil fuel driven vehicles which has not yet been replaced by a more modern solution is the 12V lead-acid battery. This is about to change, due to the emergence of alternatives to the lead-acid battery in terms of energy storage. An alternative to the lead-acid battery is the supercapacitor, which is a relatively new technology in this context. By monitoring and controlling the voltage level of the supercapacitor with a comparator circuit and a DC/DC converter, the combination can act as a substitute to the conventional 12V lead-acid battery in hybrid vehicles. The solution works to satisfaction and in combination with a support battery of preferred technology it will fulfill all current requirements and functionalities, while occupying a smaller volume of the vehicle.

Keywords: lead-acid battery, supercapacitor, comparator, DC/DC converter.

Acknowledgements

I would first like to express my gratitude towards my supervisors Björn Lövhammer, System Manager, and Alexander Engström, System Engineer, of CEVT AB for coming up with the idea and for, in such short notice, enabling me to start the project.

I would like to acknowledge Linus Franzén, Test Engineer, of CEVT AB for his contributions in the measurement phase. Along with Björn Isaksson, Senior System Engineer, and Jonas Rinman, Hardware Expert, of CEVT AB for taking their time to answer my questions regarding the circuit design and simulation phases of the project.

Finally, I would like to thank Mats Erik Setterberg of Multiguard Electronics AS for taking his personal time to help me with the design of a PCB for the comparator circuit.

Eric Rudervall, Gothenburg, November 2018

Abbreviations

AGM	Absorbed Glas Mat
BBM	Brake Boost Module
BJT	Bipolar Junction Transistor
BOM	Bill of Materials
BSG	Belt Starter Generator
CEVT	China-Euro Vehicle Technology
DAU	Data Acquisition Unit
ECU	Electronic Control Unit
EPAS	Electronic Power Assisted Steering
ICE	Internal Combustion Engine
MOSFET	Mexal-Oxide Semiconductor Field-Effect Transistor
OP AMP	Operational Amplifier
PCB	Printed Circuit Board
SHDN	Shutdown
USB	Universal Serial Bus
VDDM	Vehicle Dynamic Domain Module

Contents

1
Introduction

1.1 Background

As fuel economy becomes a more important and debated topic, some vehicles programs are moving over to either mild hybrid, full hybrid or fully electric drive trains. In practice this means that in addition to the 12V board net, there will always be an additional voltage net present in the vehicle. For mild hybrids this is typically 48V, full hybrids 400V and electric vehicles 400V – 600V. With electric drive trains, additional batteries are included in the electrical system, which often contains several times more energy than a conventional starter battery. Thus, the need for 12V energy storage has been questioned and several investigations have started to analyze whether it is possible to replace or remove it. Due to the technological advancement of supercapacitors as well as a considerable reduction in cost and volume, this technology is considered promising for this application, given that the energy storage properties of the 12V lead-acid battery can be solved.

1.2 Aim

The aim with this thesis is to develop an alternative to the traditional 12V lead-acid batteries. A power electronics circuit that charges the supercapacitors directly from the 48V battery in the 'mild hybrid' vehicles will be constructed and tested. Focus will be on fulfilling the main functions of the 12V battery in the electrical system while also fulfilling the electrical requirements on the 12V battery as a power supply.

The outcome of this thesis would eventually, if proven plausible, be integrated in the 48V vehicles after some adjustments to fulfill automotive requirements and standards.

1.3 Problem description

As the automotive industry advances in technology, additional components of varying functionalities are implemented into the vehicles and most commonly into the 12V electrical system. This results in a continuously decreasing available packing volume within the vehicle, to thwart this ongoing process some functionalities are merged into the same casings. The conventional 12V lead-acid battery has not been merged with any other components, and probably never will. But its size, cost

and environmental effect when mining the metals makes for optional solutions to be explored. One of these solutions could be a supercapacitor combined with a charging circuit, consisting of a step-down DC/DC converter and a comparator circuit that determines the upper and lower operation voltages, later known as the voltage thresholds.

In order to determine if the suggested combination of components is a viable option to the lead-acid battery the following tasks were executed:

- Compile a list of the electrical requirements on the 12V lead-acid battery, sort them in order of relevance and possibility of fulfilling.
- Determine the primary layout of the different parts of the project, build the circuit in the software and simulate tests to verify that it fulfills the requirements.
- Construct a hardware prototype and verify that it fulfills the requirements.

1.4 Scope

The work concluded in this report will not result in an industry ready product but will rather be considered as a proof of concept solution. It will prove that a power electronics circuit combined with supercapacitors can replace the 12V lead-acid battery while maintaining and fulfilling most of the main functions and electrical requirements that the battery has.

Generally the 12V lead-acid battery is considered to have four functions in today's vehicles; Providing energy for sleep functions, sufficient power to 12V starter motor, back-up power during DC/DC failure and transient current support during heavy load situations. The second function mentioning 'sufficient power to 12V starter motor' will not be considered as there are system solutions without the starter motor which has a simpler circuit layout in the 48V mild hybrid vehicle.

An assumption that had to be made, was that there will be at least one additional power source present in the vehicle, a 48V battery. Energy from this battery will be used to maintain the desired voltage and energy levels of the supercapacitors in order for them to supply the 12V electrical system in the different scenarios.

2
Theory

This section will present the necessary theoretical knowledge in order to grasp the methods and results presented in this thesis.

2.1 Capacitor

A capacitor is an electrical component that, through an electrostatic field, stores energy. It normally consists of two, or more, plates of opposite polarities that are separated by a dielectric material. There are several different types of capacitors, where factors as geometry and dielectric isolation material make them unique.

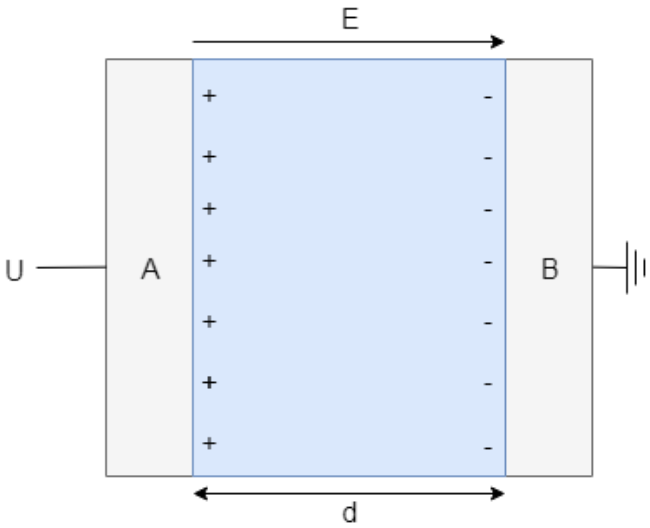

Figure 2.1: A parallel plate setup with an isolating medium in between.

In order to determine the capacitance of a parallel plate capacitor as the one in Figure 2.1 a derivation starting in

$$C = \frac{Q}{\Delta V} \tag{2.1}$$

is presented. Since the potential difference (ΔV) in a capacitor can be written as the electric field multiplied by the distance between the plates the following is given

$$C = \frac{Q}{Ed}. \tag{2.2}$$

The electric field across the insulating medium can be written as the conductivity divided by the absolute electric permittivity. The conductivity of the medium can be written as the energy divided by the area, by replacing these in (2.2) the following is given

$$C = \frac{Q}{\frac{\sigma}{\varepsilon_0}d} = \frac{Q}{\frac{\frac{Q}{A}}{\varepsilon_0}d} = \varepsilon_0 \frac{A}{d}. \tag{2.3}$$

The capacitance can also be calculated using (2.1) and replacing the energy with the instantaneous current multiplied by the time, which results in the following

$$C = i\frac{\partial t}{\partial U}. \tag{2.4}$$

(2.4) can be used to calculate the current, time or voltage for the rated capacitance of the supercapacitor.

2.1.1 Supercapacitor

The 'supercapacitor' is an energy storage alternative to the conventional battery that is well suited for applications that require short-time energy pulses and situations where energy needs to be instantly stored from motion. The supercapacitor is in an electrochemical capacitor that can store a large amount of energy. [7]

A supercapacitor can consists of several units connected in series and parallel, where two different layouts are presented in Figure 2.2 a and b. Circuit a consists of five supercapacitors connected in series and circuit b consists of two parallel branches each with five supercapacitors in series.

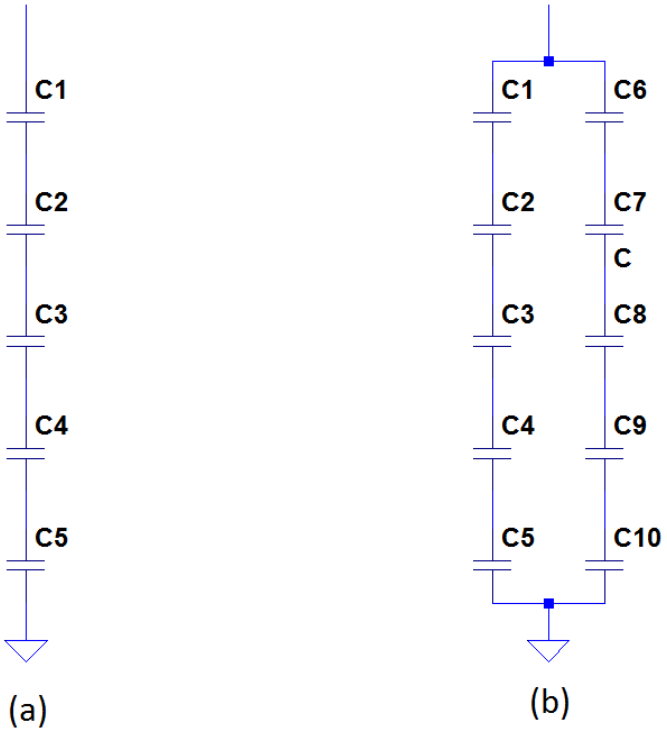

Figure 2.2: Circuit diagrams for two supercapacitor types.

Based on the specifications of each capacitor in terms of voltage rating and capacitance, type a or b is used to reach the desired voltage level and total capacitance. The total capacitance for the supercapacitor unit in Figure 2.2.a can be calculated by combining

$$C_{tot_a} = C_{series} \tag{2.5}$$

and

$$C_{series} = \frac{1}{\frac{1}{C_1} + \frac{1}{C_2} + \frac{1}{C_3} + \frac{1}{C_4} + \frac{1}{C_5}} \tag{2.6}$$

where C_{series} for a branch can be calculated using (2.6).

To calculate the total capacitance of the supercapacitor in Figure 2.2, which consists of two parallel branches of five supercapacitor units in series, (2.6) for each of the branches is summed up

$$C_{tot_b} = C_{Series1} + C_{Series2}. \tag{2.7}$$

2.2 Transistors

The transistor is an electronic device used in various industries, where control, calculations or amplifications is required. A transistor can be used as a switch or an amplifier, where the primary option is used in this thesis [6].

2.2.1 MOSFET

A Metal-Oxide Semiconductor Field Effect Transistor, also known as a MOSFET, is a power electronics switch that is widely used in the automotive industry.***REFERRERA*** The MOSFET is a voltage controlled switch, which is turned on when the Gate to Source threshold voltage V_{th} is surpassed [4].

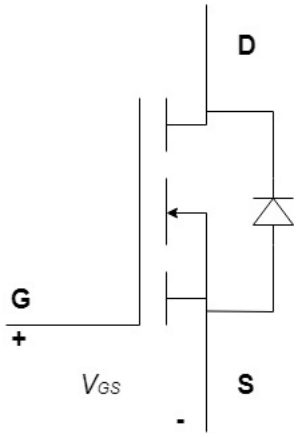

Figure 2.3: MOSFET device symbol.

Compared to other switch technologies and types, the MOSFET is considered to be optimal for low power, high switching frequency applications. There are both P- and N-channel types of the MOSFET transistor, which basically determines if it will be conducting when the voltage is $+V_{th}$ or $-V_{th}$ [4].

2.2.2 BJT

The bipolar junction transistor is used in various different industries.**REFERERA** There are two main types of bipolar transistors, NPN and PNP. Which determines when the transistor is conducting,when the current is flowing towards the base or There are two main types of bipolar transistors, NPN and PNP. The difference is the doping of the semiconducting material regions, where the NPN has two n-doped regions with a thin p-doped region in the middle, vice versa for the PNP type.

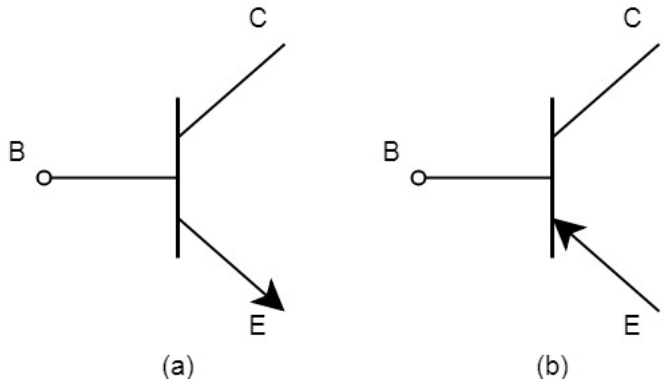

Figure 2.4: BJT device symbols for NPN (a) and PNP (b).

The collector and emitter are the power terminals of the BJT while the base is the control terminal, which means that in an NPN bipolar junction transistor current will flow from the collector to the emitter when a positive current is flowing towards the base. The NPN transistor will conduct when a positive current is flowing towards its base and PNP when the current flows in opposite direction, see Figure 2.4 for the device symbols of the two types.

2.3 Batteries

The ability to store energy electrochemically in a device known to many as a battery has simplified the technological advancement in several areas such as the portable electronics industry (cellphones, watches, calculators etc) and the electric car industry. If not for a portable source of energy all electrical devices would have to be connected to a continuous energy source, for example the electricity grid supplying the cities and such. Hence the possibility to drive a vehicle electrically would not exist if not for batteries.
There are several different battery technologies used in the automotive industry, with each technology having advantages and disadvantages. Most commonly used are the lead-acid batteries, with several sub-types, along with the Li-Ion batteries.

2.3.1 Lead-Acid Batteries

The conventional 12V battery that is used in the automotive industry is the lead-acid battery [referens]. It is favored due to its electrical characteristics of a low internal resistance enabling for a high inrush current to supply the starting sequence of the starter motor. A 12V lead-acid battery has several important functions in the electrical system of a vehicle, it
There are several different technologies used within the lead-acid battery types, where the flooded and sealed are the two main technologies. Within the vehicles both types are commonly used, where the flooded and sealed subtype 'AGM', Absorbed Glas Mat are the most common ones.

2.3.2 48V Battery

In most cases, the mild hybrid vehicles the energy source is a Li-Ion battery rated at 48V. This battery will in this thesis be considered as the only main source of energy, as the supercapacitor will be charged from this battery and then support the 12V electrical system.

2.4 Converters

In this section the converter type which is used in the circuit, some basic knowledge and functionality will be presented.

2.4.1 Buck converter

The buck converter is a so-called step-down converter, which means that the voltage supplied on the input side will result in a lower voltage on the output side, while the power level is maintained. There are two different states in this converter; switch on and off. These two can also be referred to as time intervals, where the first time interval goes from 0 to DT, which is when the switch is ON, while the second interval goes from DT to T, which is when the switch is OFF. The circuit is presented in Figure 2.5.

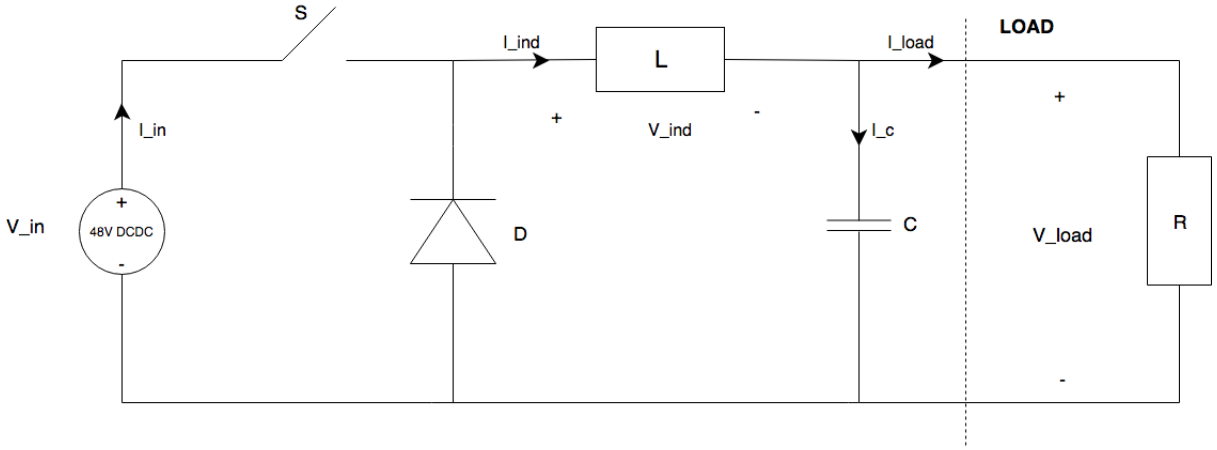

Figure 2.5: Simplified circuit for a buck converter.

3
Electrical System

In this chapter the 12V electrical system and its components in various types of hybrid vehicle solutions will be described. The 12V system across the different hybrid types has a very similar electrical architecture. It mainly consists of four components, the conventional lead-acid battery, continuous and transient loads and a DC/DC converter.

3.1 Traditional electrical system

The electrical system within the vehicles differ depending on if it is an hybrid or not. A conventional 12V vehicle usually has one main battery and one support battery, both of lead-acid type. While the 48V hybrid vehicle has one main battery on the 48V side and one on the 12V side. Since the thesis only considers the 48V hybrid electrical architecture this is the one considered as the traditional electrical system from now on. In Figure 3.1 the electrical system is presented.

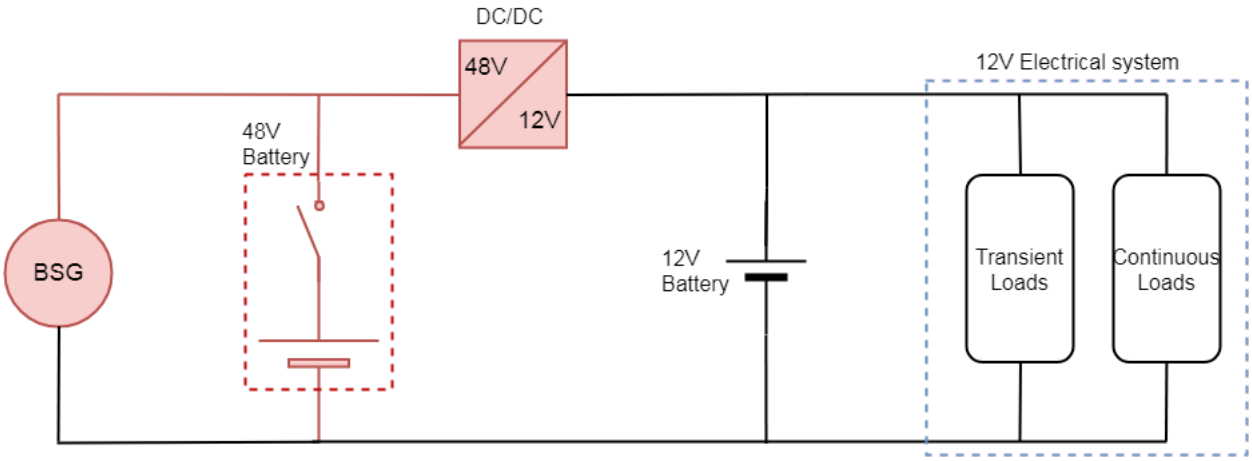

Figure 3.1: The traditional 48V electrical system architecture.

3.2 System requirements

In order to properly design the circuit to fullfil the desired functionality a list of system requirements was set up. These requirements were used as frames for the project when considering voltage and current. The list contains requirements regarding voltage levels, maximum power deliverance and maximum quiescent current

consumption. The best case scenario was for the project to fulfill all the functionalities of the 12V lead-acid battery, but that was not a likely outcome due to the lower energy content of the supercapacitor compared to a conventional lead-acid battery.

3.3 Energy sources

Previously the only energy source within the vehicles has been batteries of different types, but as of lately the supercapacitor technology has been introduced in the electrical systems in the automotive industry, with the purpose to provide energy in transient situations. An idea for this project is to investigate if the supercapacitor can be used to continuously supply the low power loads on the 12V side of the electrical system in the vehicle (a combined total current of maximum 5A), hence 60W. While also supplying the 12V system when the vehicle has entered abandoned mode and has a consumption of approximately $\sim 15mA$.

3.3.1 Battery

In the various hybrid vehicle solutions there are different types of batteries, ranging from the conventional 12V lead-acid battery to the 48V Li-Ion mild-hybrid battery and the 400V full hybrid battery. Batteries have been the main energy source in the electrical system for the automotive industry for a very long time, and will most definitely continue to be one of the main components in the vehicles. They are frequently used due to their ability to supply both low and high currents for longer periods of time due to their chemical construction.

Table 3.1: Information regarding lead-acid battery types [8].

Technology	Size	Cycles	Years
Flooded	H6	500	4
AGM	H6	2000	4

The average size of a lead-acid battery is 270x175x220 (LxWxH) mm, with a weight of approximately 21 kg.

3.3.2 Supercapacitor

The supercapacitor is currently used in the mild hybrid vehicles to support the 12V lead-acid battery with energy in the re-ignition sequence, when a large amount of current is required to reignite the ICE. The supercapacitor that is used in this project is an automotive supercapacitor module rated at 120F. It consists of five 600F supercapacitor units rated at 3V each connected in series, which gives a total capacitance of 120F according to (2.6). The layout of the module in the simulation software can be seen in Figure 3.2.

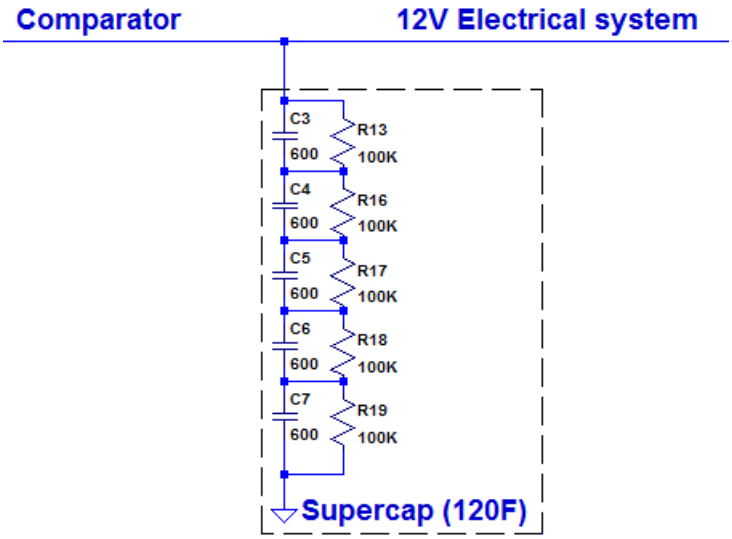

Figure 3.2: Circuit for the supercapacitor.

The $100k\Omega$ resistors in parallel with each level in the supercapacitor smooth-ens out the voltage distribution when simulating so that it is equal over all separate supercapacitor units within the module. The resistors are not present in the real life module. A supercapacitor has a very high number of life cycles compared to a lead-acid battery. In this thesis the number of cycles used when comparing is 500 000, which is half of the rated number given in a data sheet for a manufacturer of supercapacitors. The life cycle number is dependent on temperature and the instantaneous power drawn amongst more factors [9].

The average size for a supercapacitor module with the PCB circuit encapsulated is 120x130x80 (LxWxH) mm, with a weight of approximately 1.6 kg.

3.4 DC/DC Converter

All hybrid vehicles have a large energy storage in form of either a 48V or a 400V battery. Most loads in the 48V mild hybrid vehicles are on the 12V side of the electrical system, hence a step-down DC/DC converter is vital for the vehicle to deliver the desired functionality. The DC/DC converter transforms from 48V to 12V and is very large in comparison to the one used in this thesis to charge the supercapacitor module, several kilowatts compared to 75 watts.

As the ICE is on, the DC/DC will be supplying the 12V electrical system with energy, hence the 12V lead-acid battery is only in the system to assist during eventual accidents or activation of high current transient loads. In the ICE start-sequence the energy is drawn from the 48V battery, hence the applications for which the 12V lead-acid battery is required has been reduced in mild hybrid vehicles due to the 48V battery and the DC/DC converter.

3.5 Loads

When considering loads, the 12V side of the vehicles electrical system is only considered, as the product developed will only be supplying loads on the 12V system. In the system there are both continuous and transient loads, where the continuous loads have a lower but steady power consumption compared to the transient loads which consumes a large amount of power for a very short period of time.

3.5.1 Continuous loads

Loads regarded as continuous are those that consume power over a long period of time, these are usually small ECU's that control functions that need to be active continuously. Subsystems that can be considered as continuous loads are active safety, climate, exterior- and interior lights along with the powertrain and 12V USB and power outlets.

3.5.2 Transient loads

Transient loads are the ones that, for a short period of time, consume a lot of power. Subsystems that can be considered as transient loads are for example the BBM, the EPAS or the VDDM, which all three consume a lot of power during evasive manoeuvre situations.

3.6 Desired electrical systems

The electrical architecture if the supercapacitor and associated components are implemented into the 12V side of the electrical architecture depend on if the concept will be able to fully replace the 12V lead-acid battery or not. If not a small support battery will be connected in parallel with the supercapacitor. The system with just the supercapacitor can be seen in Figure 3.3.

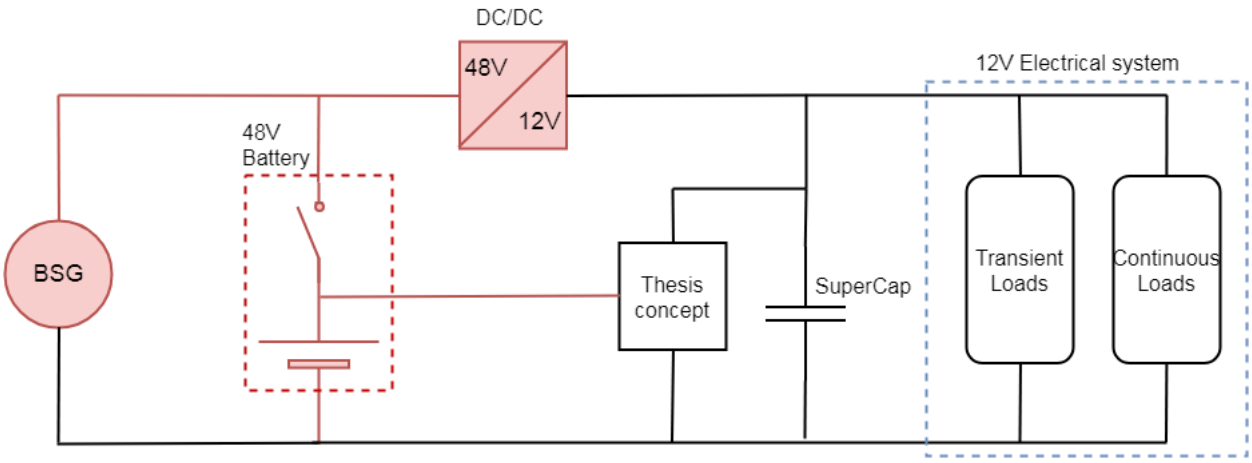

Figure 3.3: The 48V electrical system architecture if only supercapacitor is used.

While the system with the support battery connected in parallel can be seen in Figure 3.4.

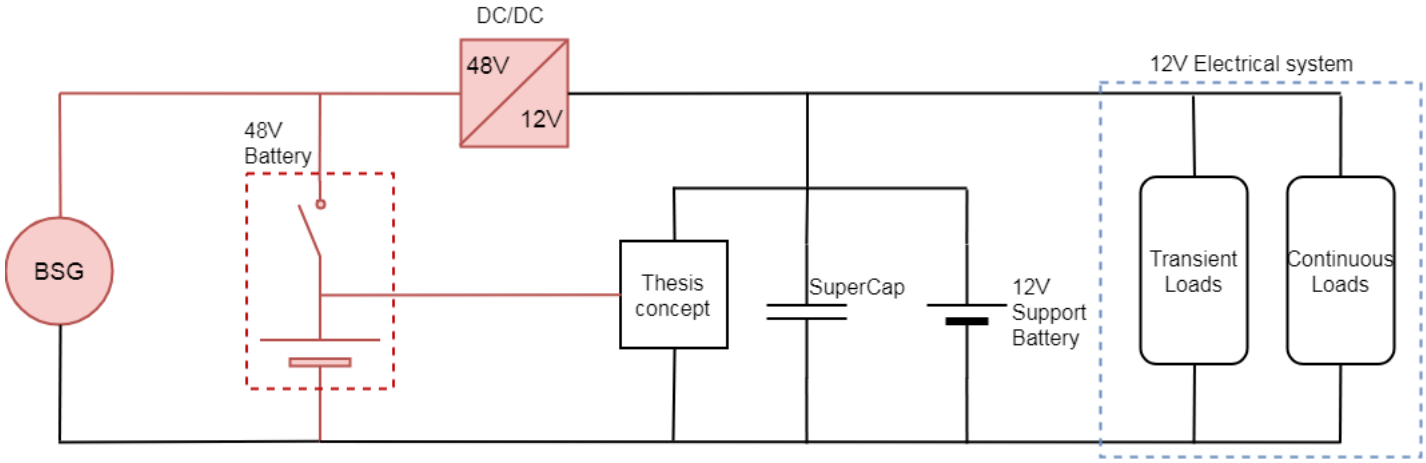

Figure 3.4: The optional 48V electrical system architecture if supercapacitor and support battery is used.

4
Methods

In this chapter the course of action is presented, from the system requirements to the circuit design, simulations and finally physical measurements.

4.1 Electrical system requirements

Since the desired outcome of this project is to be a component in future hybrid vehicles it needs to fulfill the requirements set by the surrounding electrical system. Therefore the product needs to be capable of handling voltage transients, high current drainage as well as sleep currents. The requirements will be presented in Table 4.1.

Table 4.1: Requirement list with voltage and current levels for the proposed concept.

Requirement	Description
Acceptable voltage levels	The system voltage level shall not go below X V for more than Y ms and never below Z V.
Peak transient current	The supercapacitor shall be able to deliver 235A rms for 200ms maximum and not go below 11V.
Quiescent current	The design shall be able to fully supply the vehicle in Abandoned mode.
Inactive current	The design shall be able to fully supply the vehicle in Inactive mode.
Convenience current	The design shall be able to fully supply the vehicle in Convenience mode if combined with support battery.

4.2 Circuit design

The circuit consists of three main parts; a DC/DC converter, a comparator circuit and a supercapacitor circuit. To create and simulate the circuit a design- and simulation tool called LTSpice IV was used. Partly due to its large library of industry-used components and partly since the tool was introduced and used in several courses during the education.

When designing the DC/DC converter the information given regarding the pins in the data sheet was used as a starting point. Thereafter the resistor and capacitor values were changed based on the desired operation.

The idea for the comparator circuit originates from the desired behaviour of the project. The supercapacitor is supposed to be supplying the 12V electrical system with power, and as the energy content in the supercapacitor decreases over time so will the voltage level. As mentioned in section 3.2 the 12V electrical system within the vehicle has minimum and maximum limits depending on the time elapsed during the event. The normal operation voltage for the 12V side of the electrical system range is around 12V although the system is robust and can withstand both higher and lower voltages. The voltage thresholds for the comparator are reliant on the voltage across the supercapacitor, and if it is below 11V or above 15V the comparator circuit will control a MOSFET to 'close' or 'open' respectively. Once the switch is 'closed' the DC/DC converter will charge the supercapacitor until it reaches 15V and then 'open', which isolates the DC/DC galvanically from the 12V system.

4.2.1 DC/DC Converter

As mentioned in section 2.3 the mild hybrid vehicle's main energy source is a 48V Li-Ion battery, which supplies the 12V side of the electrical system through a step-down DC/DC converter. The supercapacitor will be charged through a down-sized step-down converter that aims to have lower losses in the 'sleep current' range than the existing one.

The step-down converter used in this project is the LT3845, which is a high voltage, synchronous, current mode controller. LT3845 has an extremely low quiescent current at low loads of $120\mu A$ and a power of 75W at 15V which is equal to a charging current $I_{charge} = 5A$. Based on the information given in the data sheet regarding the programming of the pins, the resistor and capacitor values were determined.

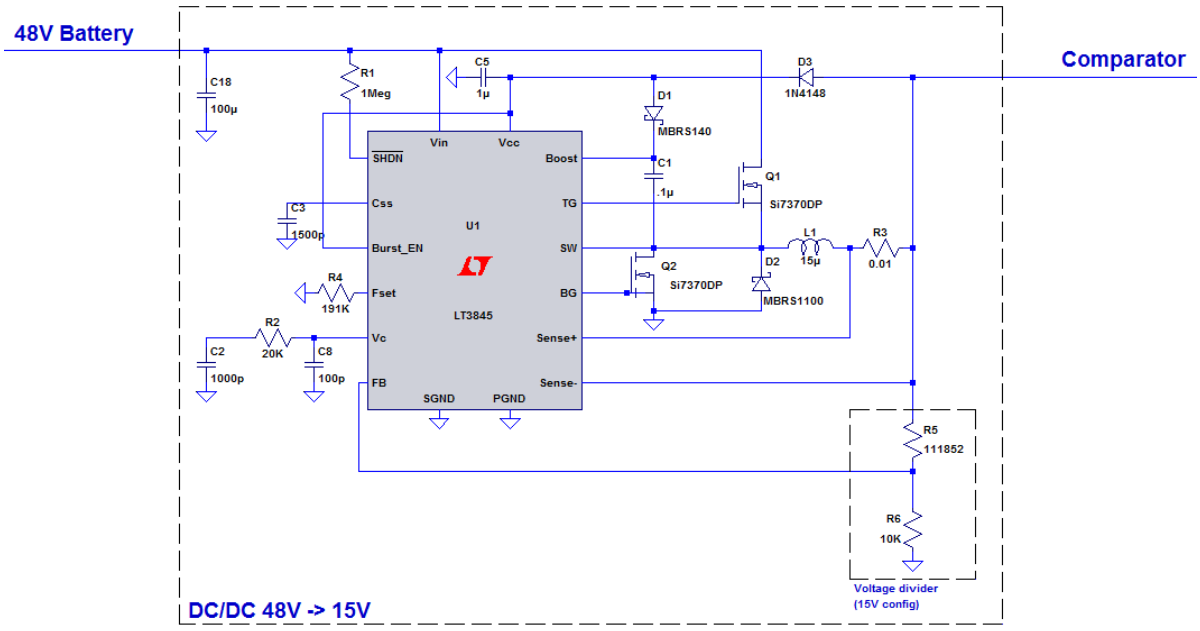

Figure 4.1: Circuit for the DC/DC Buck converter.

4.2.1.1 Pin configuration

In this section the relevant pin configurations will be presented, the entire configuration for all pins can be found in the datasheet for the LT3845 buck converter.

Vin
The V_{in} pin is the input for the DC/DC converter, it has a $100\mu F$ capacitor on the input to absorb some voltage fluctuations that may occur from the 48V battery.

Fset
Fset pin programs the oscillator frequency of the converter by an external resistor, chosen to $191k\Omega$ since that is given in the datasheet as the converter operating frequency of 100kHz.

FB
The feedback pin, dependent on the size of the resistor voltage divider connected between the output voltage can be changed to the desired value. It can be seen in Figure 4.1 that the voltage divider values are set to $120k\Omega$ and $10k\Omega$, by using

$$V_{out} = V_{in}\frac{R_2}{R_1 + R_2}. \tag{4.1}$$

Sense+ and Sense-
The positive and negative pins for the current sense amplifier measuring a 100mV across the resistor of $10m\Omega$, this results in a maximum current through the inductor L1 in Figure 4.1 of

$$I_L^{max} = \frac{U_{sense}}{R_{sense}} = \frac{0.1}{0.01} = 10A. \tag{4.2}$$

But since it is a 75W step-down converter and the output voltage will be 15V, the current will be $\sim 5A$.

4.2.2 Comparator

As the supercapacitor supports the 12V electrical system with energy it will be discharged and recharged in cycles. In order to avoid completely draining the supercapacitor and not being able to supply the electrical system with the required energy a voltage threshold that, when reached, activates the charging process is required. To avoid overcharging and potentially risk breaking the supercapacitors an upper voltage threshold is set as well, this threshold will stop the charging and isolate the supercapacitor from the DC/DC converter, hence the supercapacitor is supplying the 12V electrical system. In Figure 4.2 the entire circuit with all parts is presented.

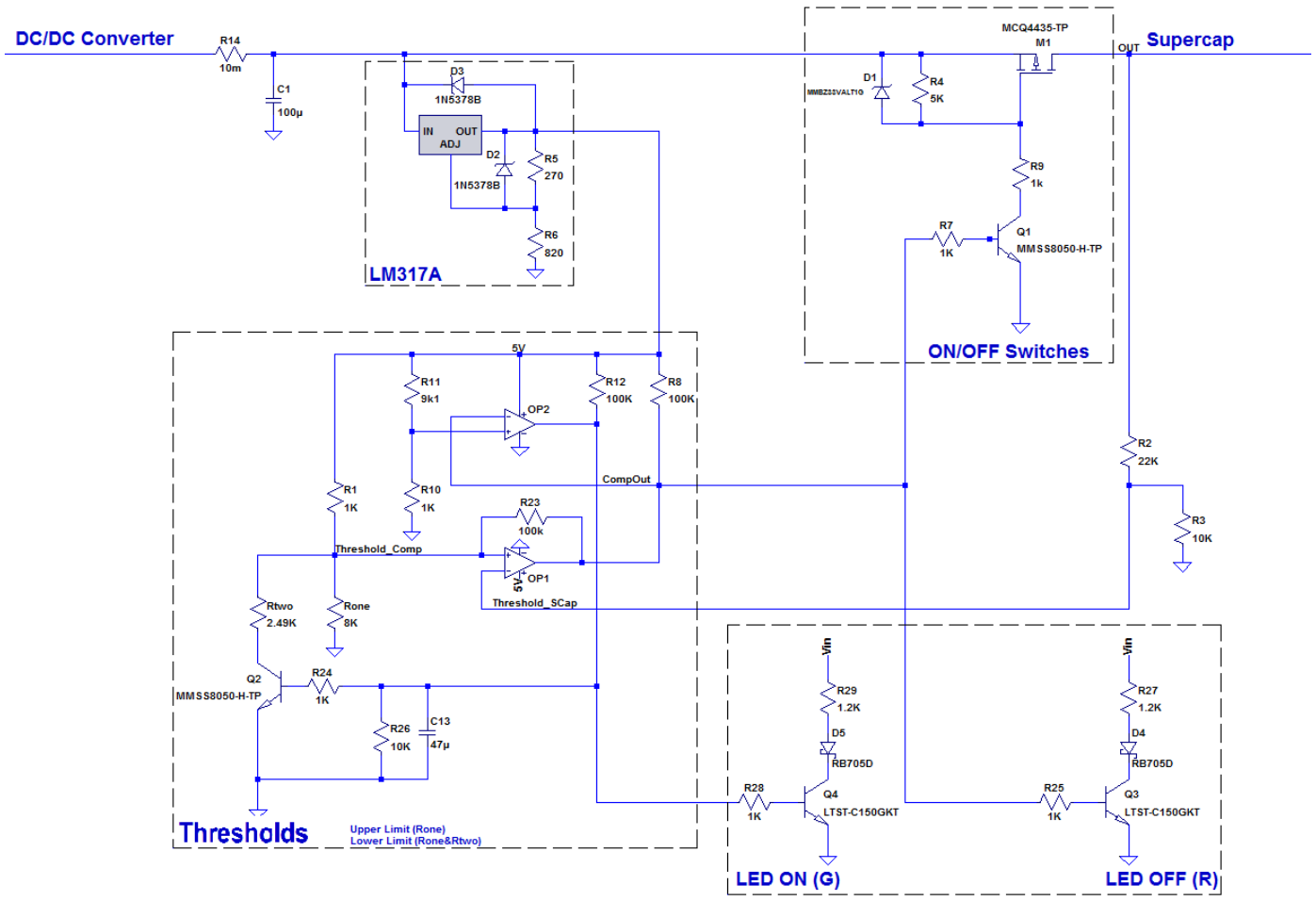

Figure 4.2: Circuit for the comparator.

In the following sections the different parts of the circuit will be thoroughly presented and described.

4.2.2.1 LM317A

This component is a linear regulator that converts the 15V input to a constant output voltage of desired value depending on the resistor values of the voltage divider on the output (R5 & R6). The output voltage will be used in the threshold part for the operational amplifiers as rail voltage and non-inverting input voltage for both OP1 and OP2.

The operational amplifiers in the comparator part of the circuit in Figure 4.2 have a supply range of 1.8V to 5.5V, which means that a 5V output from the linear regulator is a feasible option. Since the desired output voltage is 5V the equation given in the datasheet for the LM317A can be used [5]:

$$V_{out} = 1.25(1 + \frac{R_2}{R_1}) + I_{AJD}R_2 \tag{4.3}$$

As mentioned in the datasheet the adjustment current (I_{AJD}) is of $100\mu A$, which results in a very small difference. Therefore it is excluded from the equation, which then gives the following:

$$V_{out} = 1.25(1 + \frac{R_2}{R_1}) \tag{4.4}$$

Equation 4.4 combined with an E-series compatible resistance $R_1 = 270\Omega$ and the output voltage $V_{out} = 5V$ gives the following expression:

$$5 = 1.25(1 + \frac{R_2}{270}) = 1.25 + \frac{1.25R_2}{270}.$$

Which then gives the following for R2:

$$R_2 = \frac{R_1(5 - 1.25)}{1.25} = \frac{270(3.75)}{1.25} = 810\Omega.$$

The resistor value 810Ω is not in any of the standardized E-series for electrical components, hence a value of 820Ω is chosen as it is close to the calculated value. A resulting output voltage slightly higher than 5V is to be expected but the operational amplifiers, as mentioned previously, has normal operation with a voltage as high as 5.5V. Diodes D2 and D3 are used to prevent external capacitors from discharging through the regulator and potentially break it.

4.2.2.2 Thresholds

Main components in the threshold part of the circuit in Figure 4.2 are two operational amplifiers (OP1 and OP2) and an NPN-transistor (Q2).
The operational amplifier named 'OP1' compares the voltage over the supercapacitor with the voltage $V(threshold\_comp)$ in Figure 4.2 and if

$$V(threshold\_comp) > V(threshold\_scap)$$

the output signal from OP1 will be $\sim 5V$. In the opposite case, where

$$V(threshold\_comp) < V(threshold\_scap)$$

OP1 will output $\sim 0V$. In Figure 4.2 it can be seen that the voltage of the non-inverting input of OP1 is determined by a voltage divider of either $R1 + Rone$ or $R1 + (Rone//Rtwo)$ based on the state of the NPN-transistor Q2.
While

$$V(threshold\_comp) > V(threshold\_scap)$$

the transistor Q2 will not be conducting since the output from OP2 is $\sim 0V$ as the inverting input (-) is larger than the non-inverting input (+). As the relation changes and the following becomes true

$$V(threshold\_comp) < V(threshold\_scap)$$

the operational amplifier OP2 will output $\sim 5V$, consequently transistor Q2 will start conducting. As Q2 starts conducting the threshold will be lowered since the voltage divider on the non-inverting (+) input of OP1 gets an additional resistance *Rtwo* in parallel with *Rone*. In Table 4.2 the different MOSFET states are presented in relation to the voltage relation on the inputs of the operational amplifier OP1.

Table 4.2: Comparators control of the MOSFET.

Voltage relation	MOSFET state	Voltage divider
$V_{threshold\_supercap} < V_{threshold\_comp}$	On	R1 + Rone
$V_{threshold\_supercap} \geq V_{threshold\_comp}$	Off	R1 + Rone//two
$V_{threshold\_supercap} < V_{threshold\_comp}$	On	R1 + Rone

4.2.2.3 On/Off Switches

In Figure 4.2 the On/Off switches part of the circuit mainly consists of two switches, a P-channel MOSFET (M1) and a NPN BJT (Q1). As mentioned in 4.2.2.2 the operational amplifier, OP1, will output $\sim 5V$ if

$$V(threshold\_comp) > V(threshold\_scap)$$

which will result in Q1 not conducting, hence M1 is conducting and charging the supercapacitor module.

4.2.2.4 LED On/Off

The time intervals for the re-occurring stages, II and III, will be strongly dependent on the amount of current drained from the supercapacitor. If a higher current is

drawn, 4-5A, the time interval before reaching the 11V threshold can be calculated using (2.4).

4.2.3 Supercapacitor

The supercapacitor used in this project is a 120F automotive module consisting of five 600F capacitors connected in series, as mentioned in section 3.3.2.

4.3 Simulations

Due to the high switching frequency of $100kHz$ of the DC/DC converter and the considerably large capacitor, simulations of the entire system are very time consuming. Therefore the simulations have been split up into separate parts, where the charging of the supercapacitor has been executed with a fraction of the real value of the supercapacitor. The comparator circuit from Figure 4.2 was simulated with a constant 16V input instead of the DC/DC converter from Figure 4.1.

4.3.1 Charging supercapacitor

The simulations for the charging cycle of a supercapacitor of 120F shall have the same characteristics as for a $100\mu F$ or a $10F$ supercapacitor, with the only difference being the time intervals until the 15V threshold is reached and the charging stops. Therefore simulations using a supercapacitor of only $100\mu F$ were executed in a custom circuit shown in Figure 4.3, where the voltage over the supercapacitor is forced to 11V by the additional supply unit $V3$.

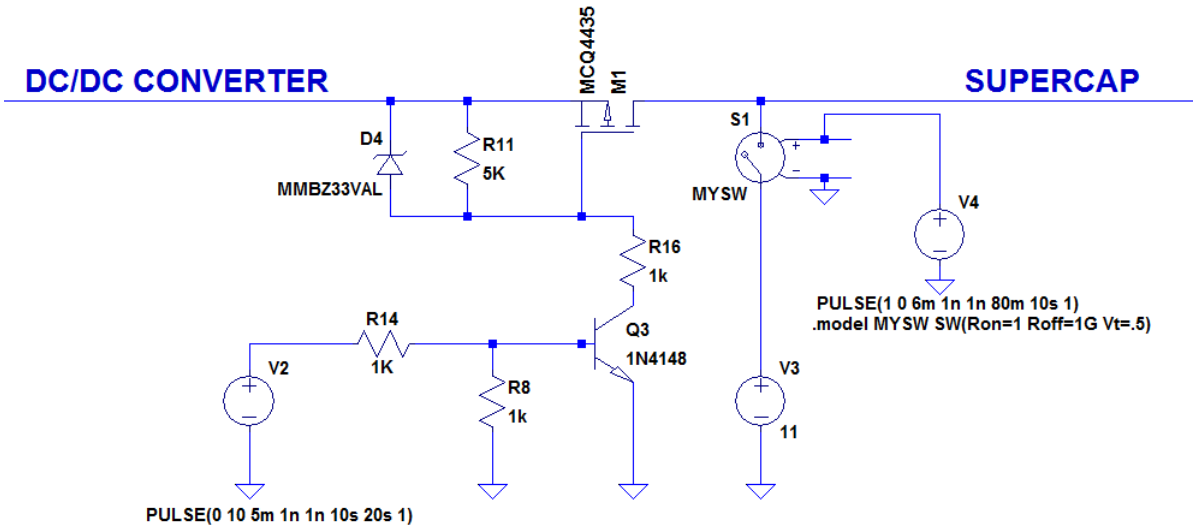

Figure 4.3: Circuit to simulate the charging of the supercapacitor from 11V to 15.

Instead of having the operational amplifiers and the comparator circuit from Figure 4.2 the circuit in Figure 4.3 is used to simulate the charging of the supercapacitor

from $11V$ to $15V$. Transistor Q3 is controlled by a voltage supply programmed to make the transistor stop conducting after $5ms$ and start the charging of the supercapacitor.

The charging of the supercapacitor will be simulated with capacitances of $C_{supercap} = 1F$ and $C_{supercap} = 10F$.

4.3.2 Control of MOSFET

In order to properly cycle the supercapacitor between $11V$ and $15V$ the MOSFET needs to open and close at the right moment, this behaviour is controlled by the comparator circuit shown in Figure 4.2. The simulations for this part of the system were conducted using a constant 16V supply instead of the DC/DC converter from Figure 4.1 due to the increased complexity of the simulation and increased simulation times. If the supplying unit was the DC/DC converter or a constant voltage supply was irrelevant since the important part of the simulation was to verify that the comparator is switching the MOSFET at the right voltage thresholds.

The energy flow in the circuit for the charging state is shown in Figure 4.4.

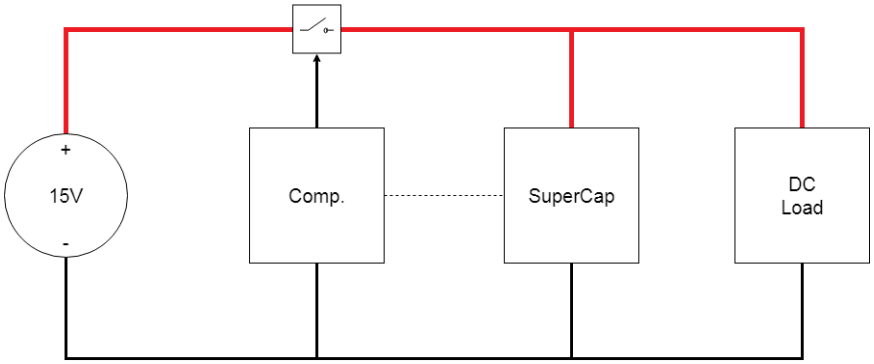

Figure 4.4: Charging state for the circuit.

The energy flow in the circuit for the discharging state is shown in Figure 4.5.

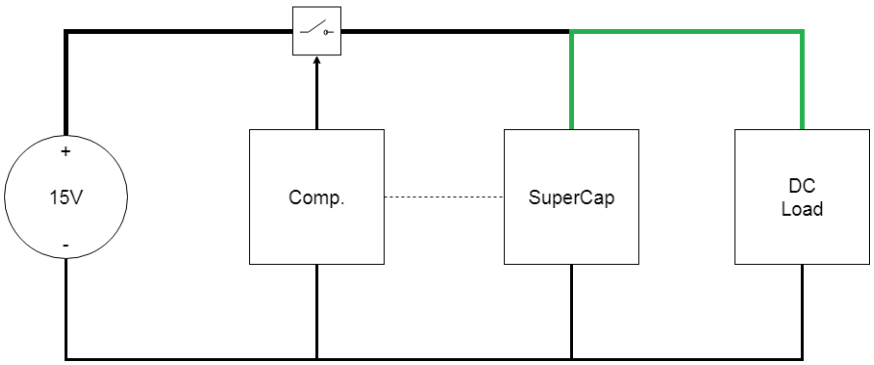

Figure 4.5: Discharging state for the circuit.

4.4 Hardware prototype

Once the design was finished and the simulations showed the desired results a PCB layout was created and the components from the design were searched for and put together in a BOM, Bill of Materials, list. In the BOM list component names, value, manufacturer, units, unit price etc were entered. All components required to create the circuit in hardware were inserted in the BOM along with some standoffs and other peripherals, every component entered with a few reserves in case of any unwanted accidents. The BOM list can be seen in Appendix 1.

4.4.1 PCB Layout

The schematic was copied from the layout constructed in LTSpiceIV while the PCB and the component layout of the circuit board was designed in a program called DipTrace, it can be seen in Figure 4.6.

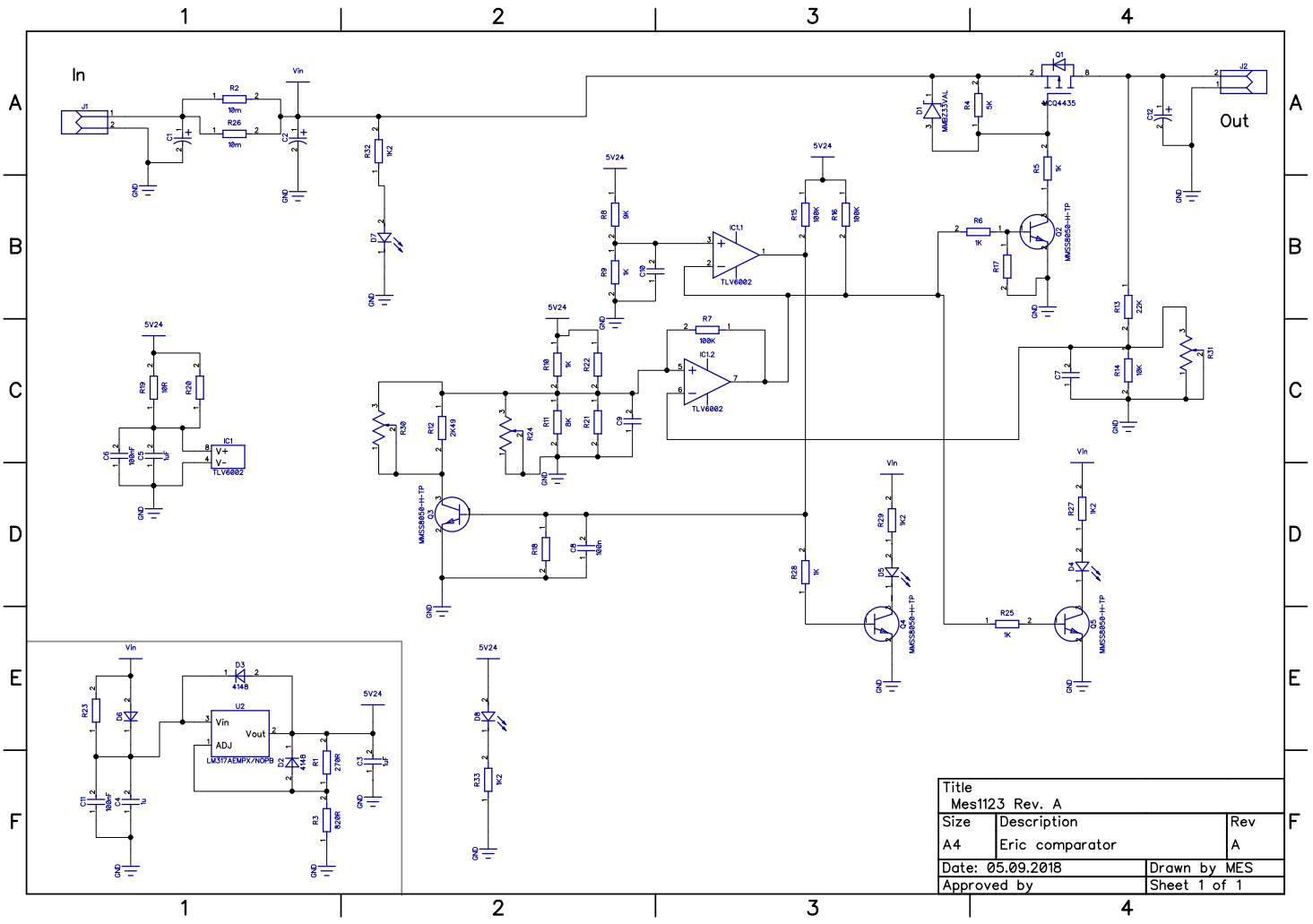

Figure 4.6: Schematic layout that was made in DipTrace.

Once the schematic was transferred the components had to be position in an optimal way in terms of heat, harmonics and consumption. Generally the most critical traces, the ones sensitive to changes in impedance or harmonics, are placed first and then built around. The circuit was designed in a clear, logical way from there on.
The finished PCB layout sent to a printing company can be seen in Figure 4.7. It is a two-layer PCB with a few through hole mounted components but mainly surface mounted components of size 1206.

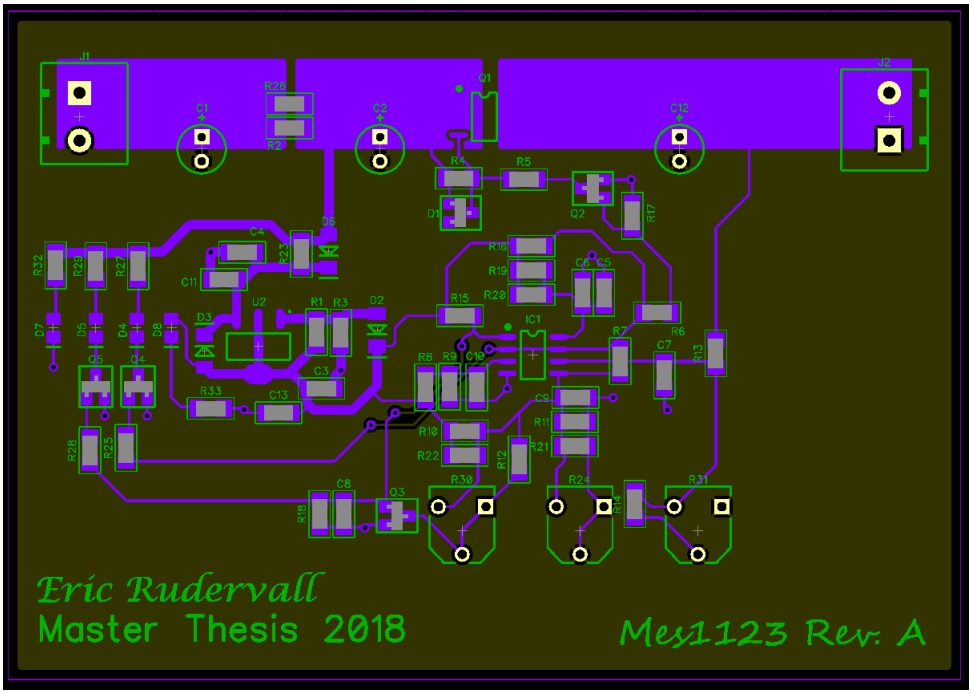

Figure 4.7: PCB layout that was sent to printing company.

The PCB is 70x100mm in size and a photo of the real PCB with components mounted can be seen in Figure 4.8.

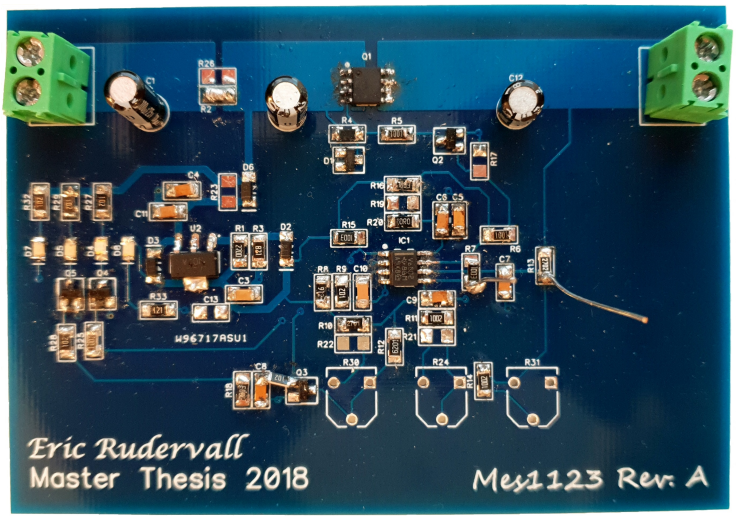

Figure 4.8: Photo of the PCB with components solder onto it.

4.5 Physical measurements

When the hardware prototype was built the testing part of the project was initiated. Several different test cases with and without the DC/DC step-down converter was planned to be performed, all to mimic real life situations. Unfortunately the purchase department at CEVT AB confirmed the approval of the order, but in fact they never placed it so the DC/DC step-down converter arrived just two weeks before the end of the thesis. So instead of testing with the DC/DC converter some tests in complete vehicle were performed.

4.5.1 Test plan

In order to properly verify the functionality of the design a set of test cases were set up together with the supervisors at CEVT, all based on real-life situations. Current consumption and voltage drops in different vehicle modes such as sleep, inactive, convenience and active mode were measured. In Table 4.3 a summary of the various test cases are presented. All test cases were started from 0V on the supercapacitor and it was charged up before the various currents were drained from it. This in order to get a continuity and simplify the analysis part where different results are compared.

Table 4.3: Test plan cases.

Environment	Test case	Sequence
Rig	Abandoned mode	Supercapacitor supplies the load with $50mA$.
	Inactive mode	Quiescent current for 20 minutes, then 4.5A for 10s.
	Convenience mode	Inactive mode sequence and then 10A for 10s.
	Test case 4	5A for 10s, then 10A until $U_{SCAP} =\sim 2V$
	Test case 5	Quiescent current 5min, then 10A until $U_{SCAP} =\sim 2V$
	Test case 6	5A continuously
	Test case 7	4.5A continuously (slow charging)
Complete vehicle	Abandoned mode	Supercapacitor supplies the vehicles 12V system.
	Inactive mode	Quiescent current for 20 minutes, then 4.5-5A for 10s.
	Convenience mode	Inactive mode sequence and then 10A for 10s.
	Active mode	Abandoned, inactive, convenience and then active mode.

4.5.1.1 Abandoned mode

For the vehicle to enter the 'Abandoned mode' it needs to be locked and left untouched for 2-3 minutes. In abandoned mode only the most vital functions needed for the vehicle to be unlocked and used at any moment are active, their combined current consumption is approximately $15mA$. It can be concluded when observing Figure 4.9 and Equation 2.4 that the only difference between different quiescent currents is the time until it reaches 11V for a specific dU. This time is linearly decreasing as the quiescent current is increased, therefore a quiescent current of 50mA was used in the rig environment instead of the 15mA as that test would take

$$dt = \frac{C}{I}dU = \frac{120}{0.05} \cdot 4 = 9600s = 2.66h \tag{4.5}$$

to conduct according to Equation 4.5 instead of the

$$dt = \frac{C}{I}dU = \frac{120}{0.015} \cdot 4 = 32000s = 8.88h \tag{4.6}$$

for a quiescent current of 15mA. The time-voltage relation for various quiescent currents are shown in Figure 4.9

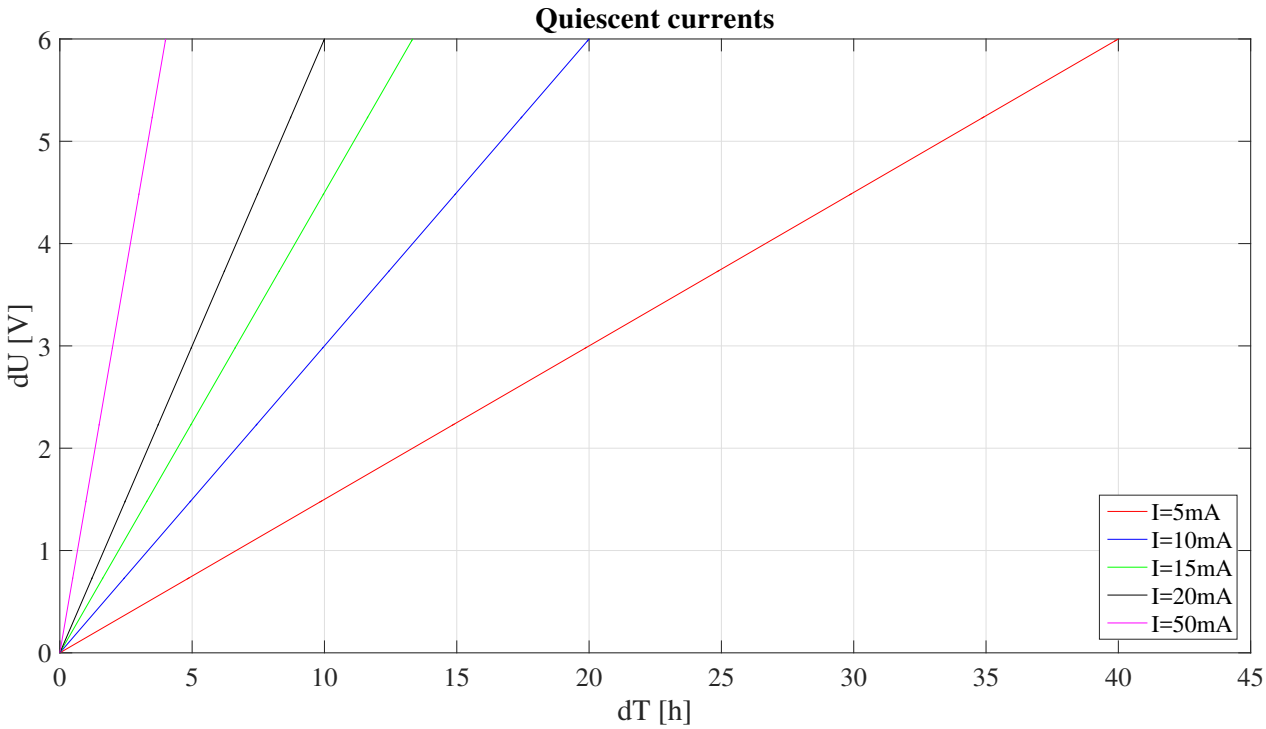

Figure 4.9: Various quiescent currents presented in a dT-dU graph.

4.5.1.2 Inactive mode

As the vehicle is brought up from 'Abandoned mode' it enters 'Inactive mode' and consumes approximately $4 - 5A$ continuously. In Figure 4.10 the times required to charge the supercapacitor (dT) for a set of five charging currents (I) and voltage differences (dU) are presented, all based on Equation 2.4.

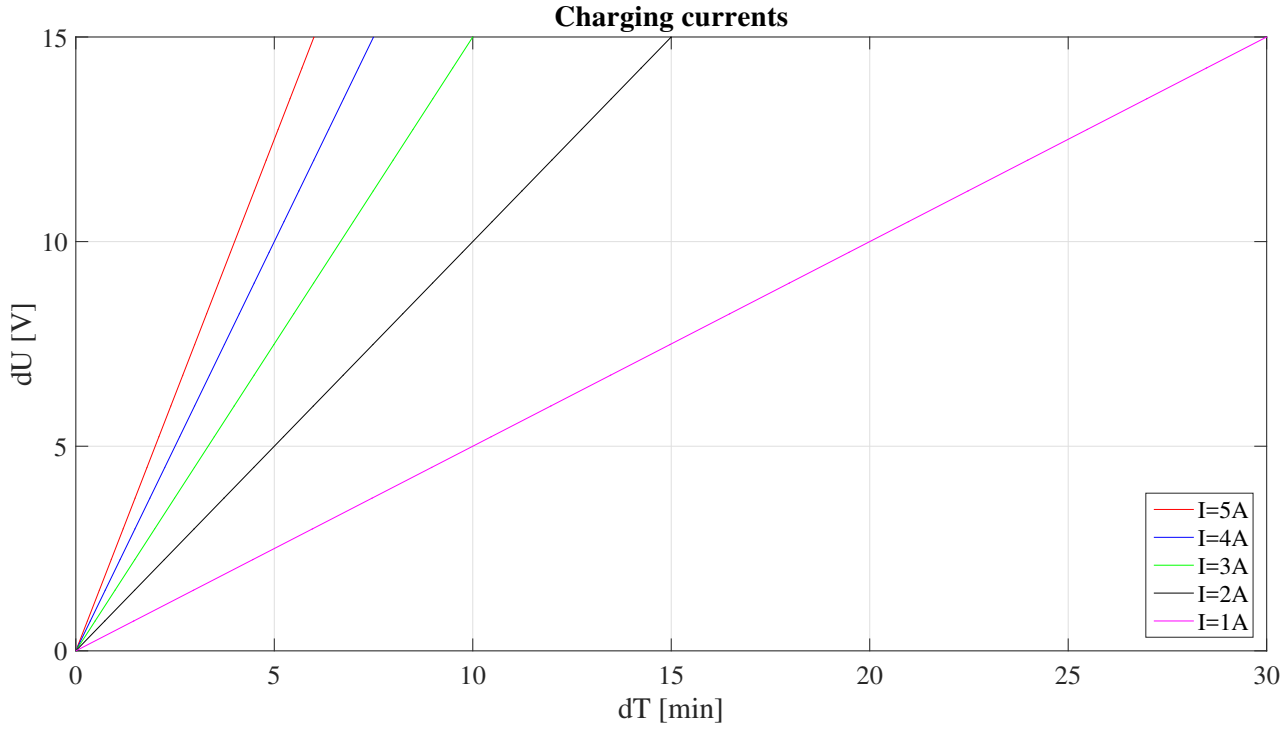

Figure 4.10: Various charging currents presented in a dT-dU graph.

4.5.1.3 Convenience mode

When the vehicle is in inactive mode and a user presses the Start button on the dashboard once the vehicle will enter convenience mode, in this mode the vehicle consumes approximately $10A$ continuously. Since the comparator circuit only charges with $5A$ this case is interesting as the voltage over the supercapacitor will decrease continuously when a current over 5A is drawn from it.

4.5.1.4 Test case 4

This case is considered to be a real-life scenario, where the user arrives and enters the vehicle, then puts it in convenience mode for a long period of time. The drainage will be started at a supercapacitor voltage of $U_{SCAP} = 15V$, which is the optimal case since it will have the most possible energy stored.

4.5.1.5 Test case 5

This case is also considered to be a real-life scenario, where the user arrives and enters the vehicle, then puts it in convenience mode for a long period of time. The

drainage will be started at a supercapacitor voltage of $U_{SCAP} = 12V$, which unlike Test case 4 is not an optimal case since it will be close to the voltage threshold of $U_{SCAP} = 11V$.

4.5.1.6 Test case 6

This case is an extension to the inactive mode case, which only consumes $4 - 5A$ for a time period of . In this case a constant current $I_{LOAD} = 5A$ will be drawn from the supercapacitor, the desired information gained from this test will be how the $5A$ current is divided between the supercapacitor and the comparator circuit.

4.5.1.7 Test case 7

In this case a DC load that consumes 4.5A continuously was applied. This level of current consumption is close to the charging current from the comparator circuit, hence an interesting case to investigate in order to evaluate the designs capability to handle 'slow charging'.

4.5.1.8 Active mode

The Active mode is the final state before the ICE is turned on, all ECUs are activated and the total current consumption is dependent on the equipment level of the vehicle. With a consumption of $\sim 10 - 15A$ to be expected.

4.5.2 Measurement equipment

To measure the voltages and currents in the physical measurements mentioned in section 4.5.1 a data acquisition unit is required, along with some current shunts and contacts. In Table 4.4 all equipment used to perform the measurements is presented.

Table 4.4: Measurement equipment used during physical measurements.

Equipment	Specifications	Miscellaneous
Yokogawa DL850EV	16 channels, 1 kS/s	Data Acquisition Unit
IT8516C+	Case based current	DC Load
Current shunt 1	5A/50mV	Used to measure I_{SCAP}
Current shunt 2	30A/50mV	Used to measure I_{LOAD}
Banana plugs	-	To connect points to DAU

Voltages were measured using custom made breakout connectors for the points V_{in} and V_{out}, while the threshold voltages $V_{SCAPThreshold}$ and $V_{Threshold}$ were measured on small conducting rods soldered to the desired pins on the PCB.

5
Results

In this chapter the results retrieved from simulations, theoretical and physical measurements will be presented.

5.1 Simulations

In this section the simulation results for the DC/DC converter in Figure 4.1, the comparator in Figure 4.2 and the supercapacitor in Figure 3.2 will be presented.

5.1.1 Comparator control

It can be seen in Figure 5.1 the comparator circuit controls the MOSFET so that when V(out) reaches 15V it opens the MOSFET hence isolating the supercapacitor from the DC/DC converter. When isolated, the supercapacitor will supply the 12V electrical system until it reaches 11V, which is the lower threshold that makes the MOSFET conducting again.

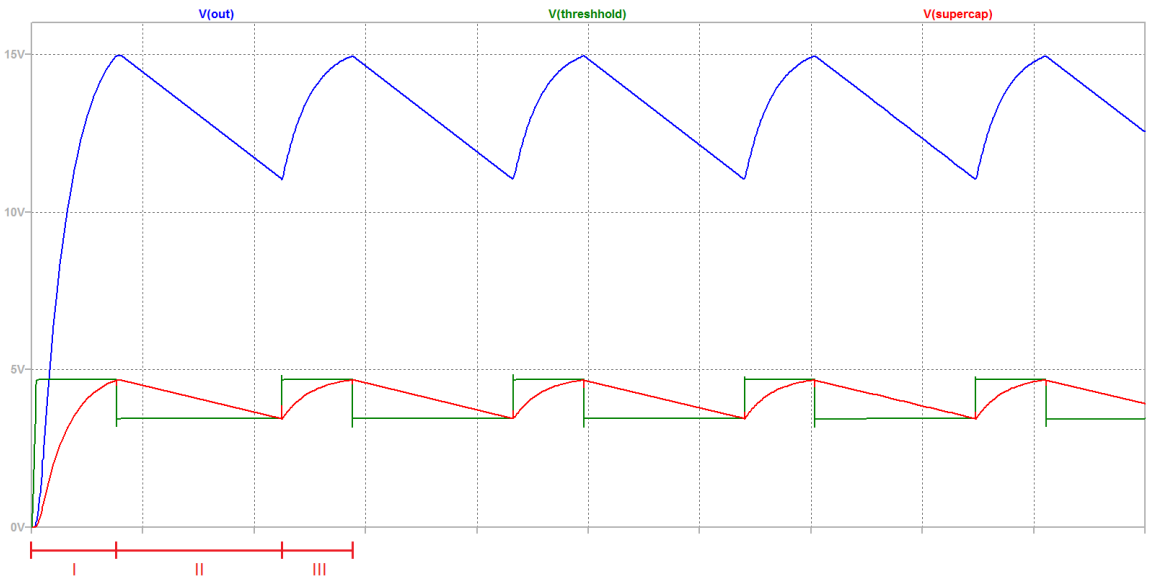

Figure 5.1: Example graph for the comparators purposed operation and control of the MOSFET.

In Table 5.1 the events in Figure 5.1 are presented and the voltage relation that determines the MOSFET states are declared.

Table 5.1: Charge and discharge stages that occur due to the comparators control of the MOSFET.

Stage	Voltage relation	Event	MOSFET State
I	$V_{supercap} < V_{threshold}$	Start-up phase	On
II	$V_{supercap} > V_{threshold}$	Discharge phase	Off
III	$V_{supercap} < V_{threshold}$	Charging phase	On

5.1.2 Charging of supercapacitor

As mentioned in section 4.3.1 two charging simulations were performed, one with a supercapacitor of 1F and another of 10F. The results for the charging of the 1F supercapacitor be seen in Figure 5.2.

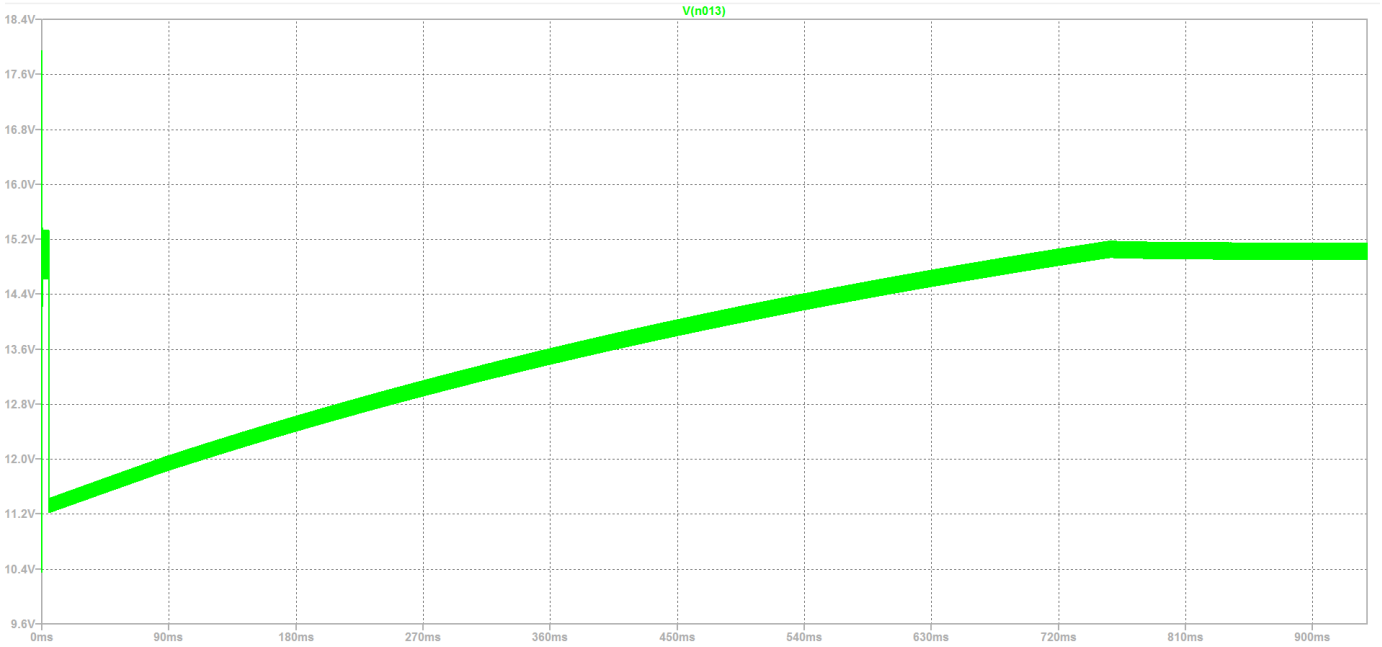

Figure 5.2: Charging of a 1F supercapacitor.

In Figure 5.2 it can be seen that the voltage at the supercapacitor is forced to 11V by the custom circuit and then recharged until it reaches 15V. The charging for the 10F supercapacitor can be seen in Figure 5.3.

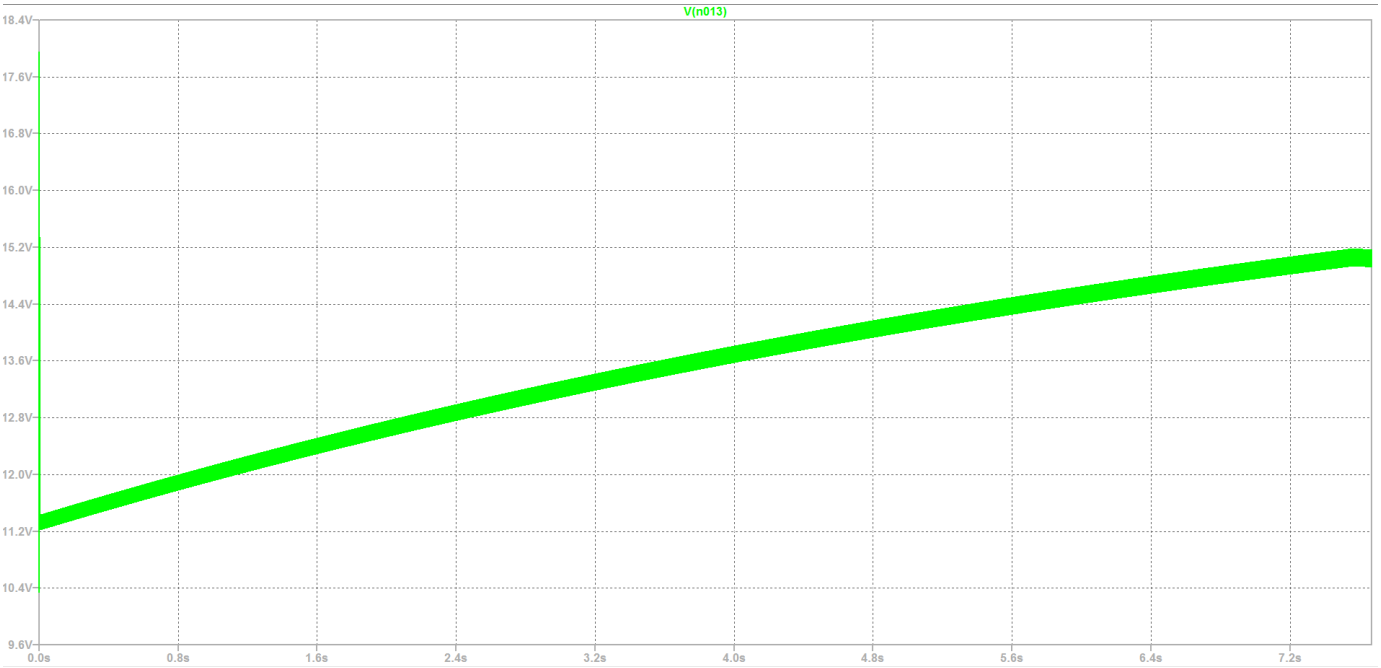

Figure 5.3: Charging of a 10F supercapacitor.

5.2 Theoretical measurement results

As mentioned in the Methods chapter the supercapacitor was charged to 15V and then the MOSFET transistor turned off and initiated the discharge phase until 11V was reached, as presented in Table 5.1. The discharge phase times are dependent on the current that is drained from the supercapacitor, the currents for the usage modes are shown in Figure 5.4.

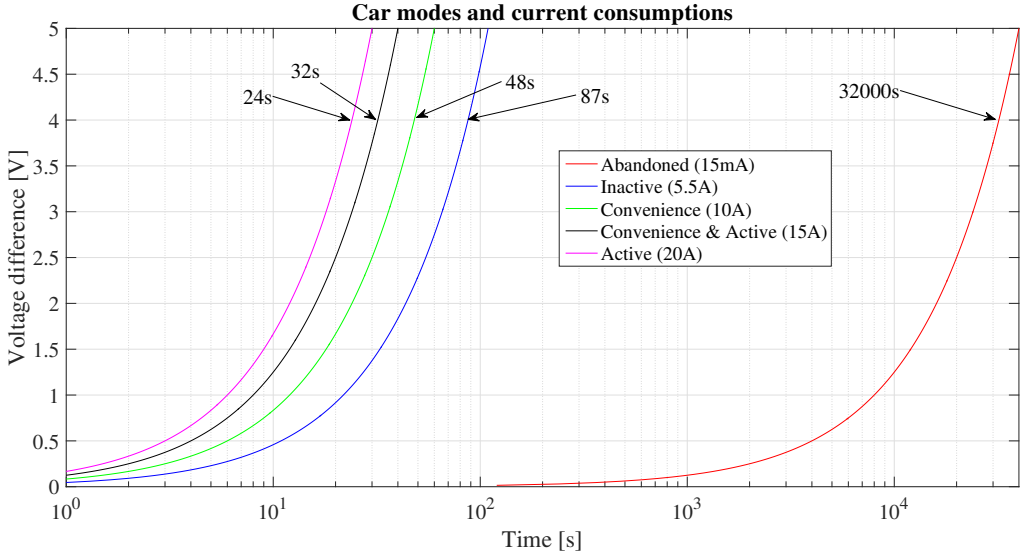

Figure 5.4: Car modes and corresponding voltage-time relations with a logarithmic X-axis.

In the convenience and active vehicle modes the current drained from the supercapacitor is larger than the current supplied by the charging circuit (5A), while it is approximately equal in the inactive mode. A net loss in energy in the supercapacitor leads to the voltage level slowly decreasing. As mentioned in Table 4.1 the lowest voltage level accepted is 9.7V for a very short period of time, therefore the case where the net supply is negative below the 11V threshold is of interest. In Figure 5.5 the time passed before the voltage decreases with 1V for the different vehicle modes can be seen.

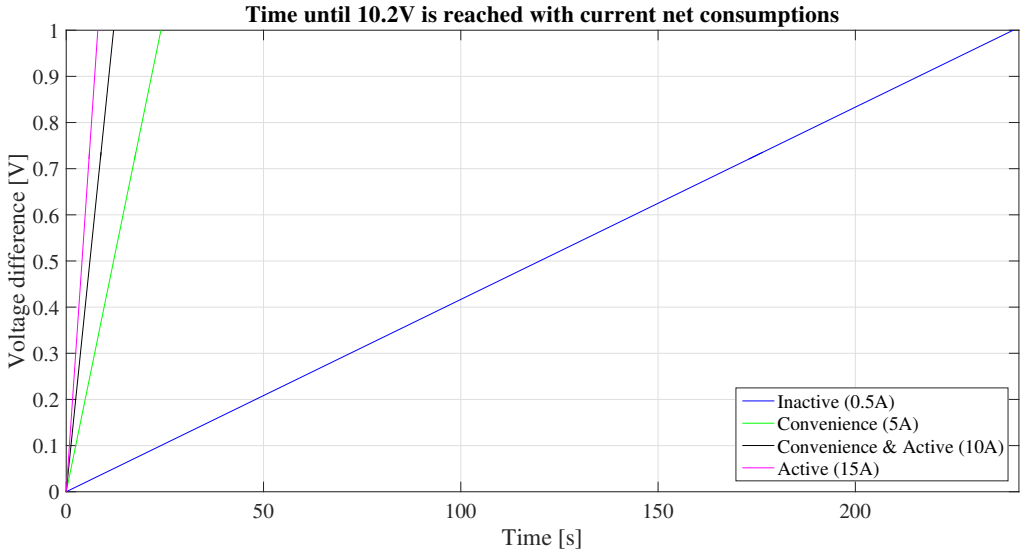

Figure 5.5: Vehicle modes with net consumption.

5.3 Physical measurements

The first seven tests in the testing phase of the project were performed according to the plan from section 4.5.1 without the DC/DC step-down converter and instead used a 15V power supply. This to verify the functionality of the comparator circuit prior to performing any tests with the DC/DC converter.

5.3.1 Measurements in rig

All graphs presented in this section are from measurements performed in rig environment. The tests performed are all presented in Table 4.3.

5.3.1.1 Abandoned mode

A test with a DC load of 50mA was performed, to mimic the current consumption in a vehicle in 'abandoned mode' without being too time consuming. Results are presented in Figure 5.6.

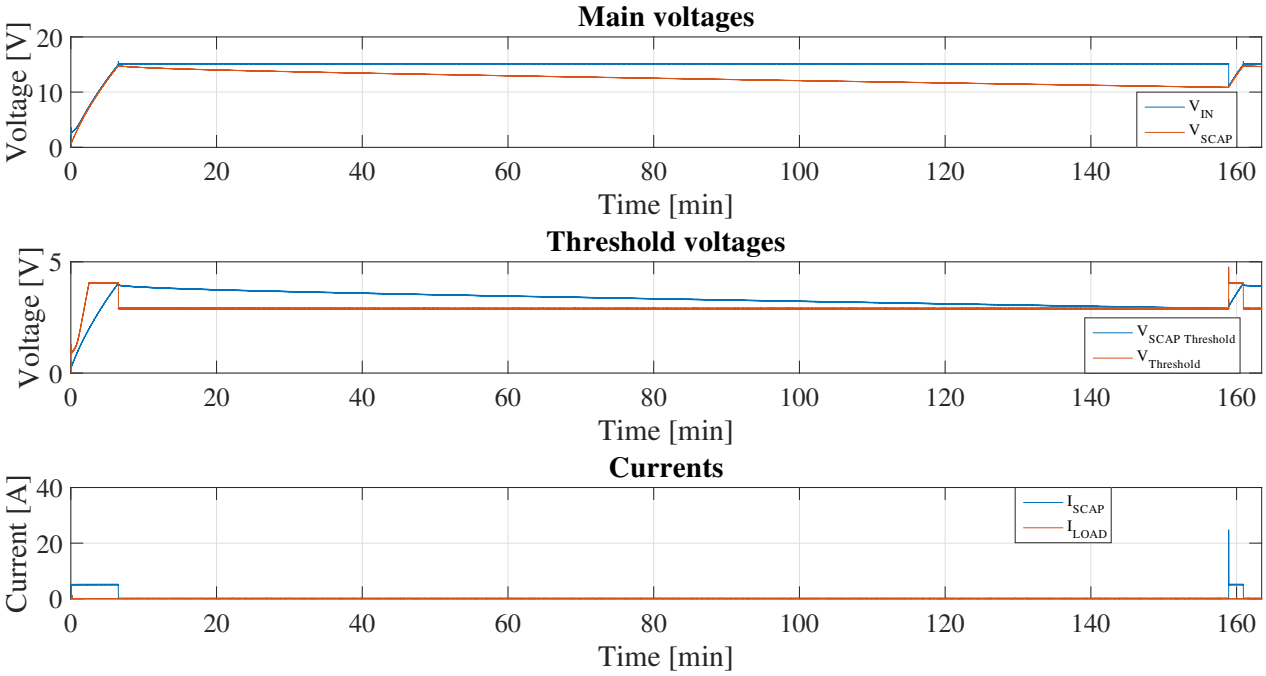

Figure 5.6: Measured voltages and currents for the abandoned mode test sequence in a rig.

A zoom in of the charging phase with similar characteristics to the one given in section 5.1.2. The zoom is on the time period around 160 minutes, where $V_{supercap}$

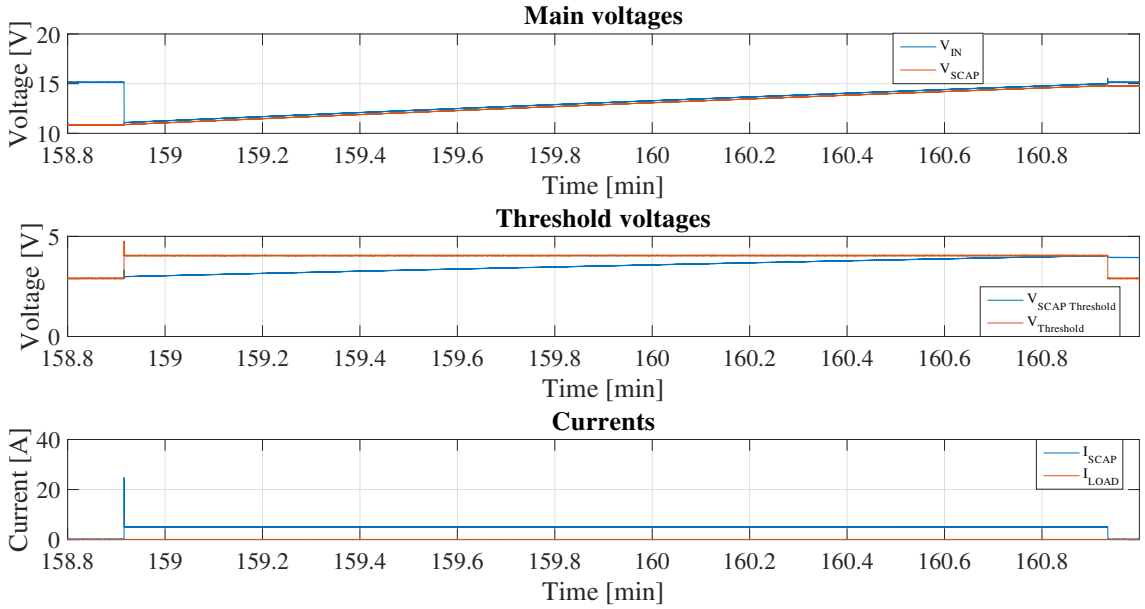

Figure 5.7: Measured voltages and currents for the zoom in of the abandoned mode test sequence in a rig.

5.3.1.2 Inactive mode

A summary of the test sequence for the 'Inactive mode' test can be seen in Table 4.3 while the extended explanation is presented in section 4.5.1.2.

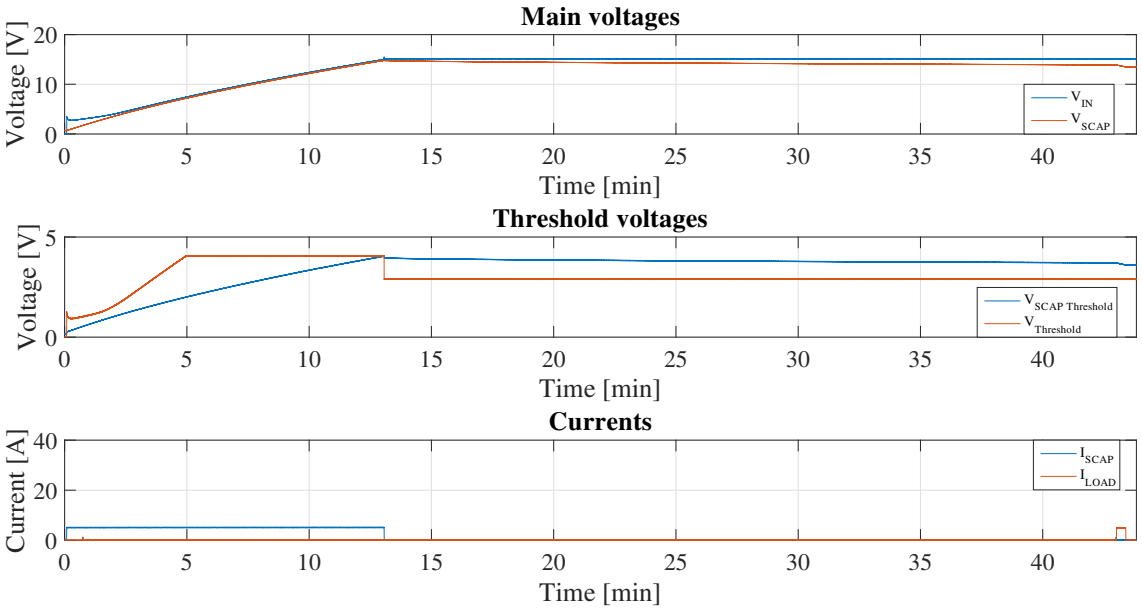

Figure 5.8: Measured voltages and currents for the inactive mode test sequence.

A zoom in of the region where the DC load is applied can be seen in Figure 5.9.

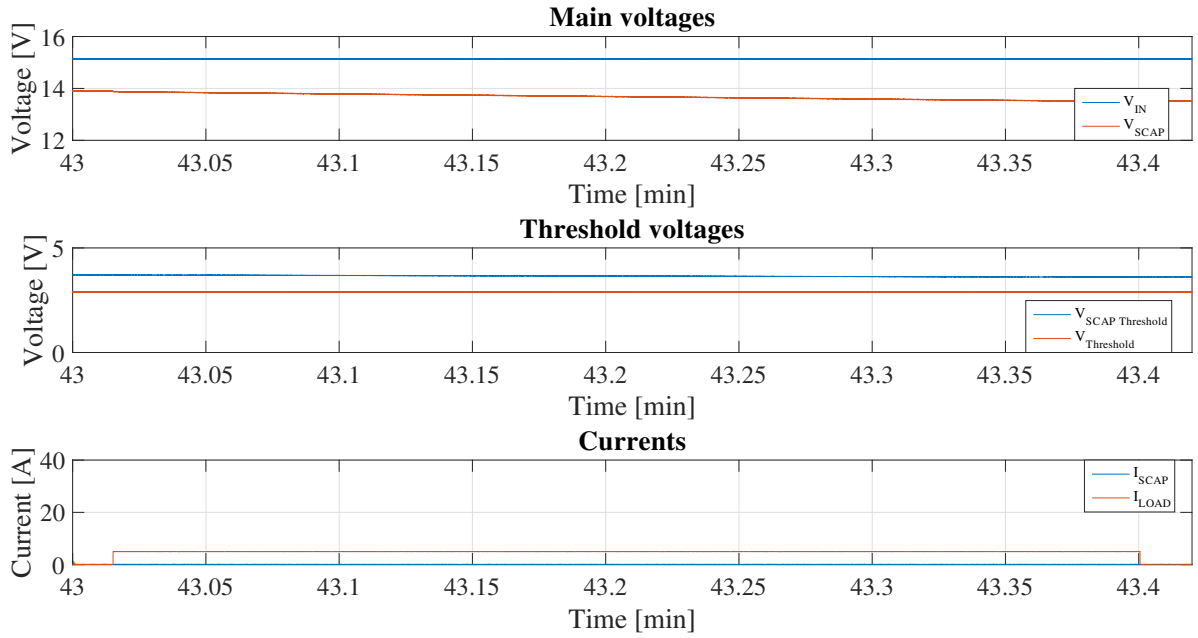

Figure 5.9: Measured voltages and currents for the inactive mode test sequence.

5.3.1.3 Convenience mode

A summary of the test sequence for 'Convenience mode' can be seen in Table 4.3 while the extended explanation is presented in section 5.3.1.3.

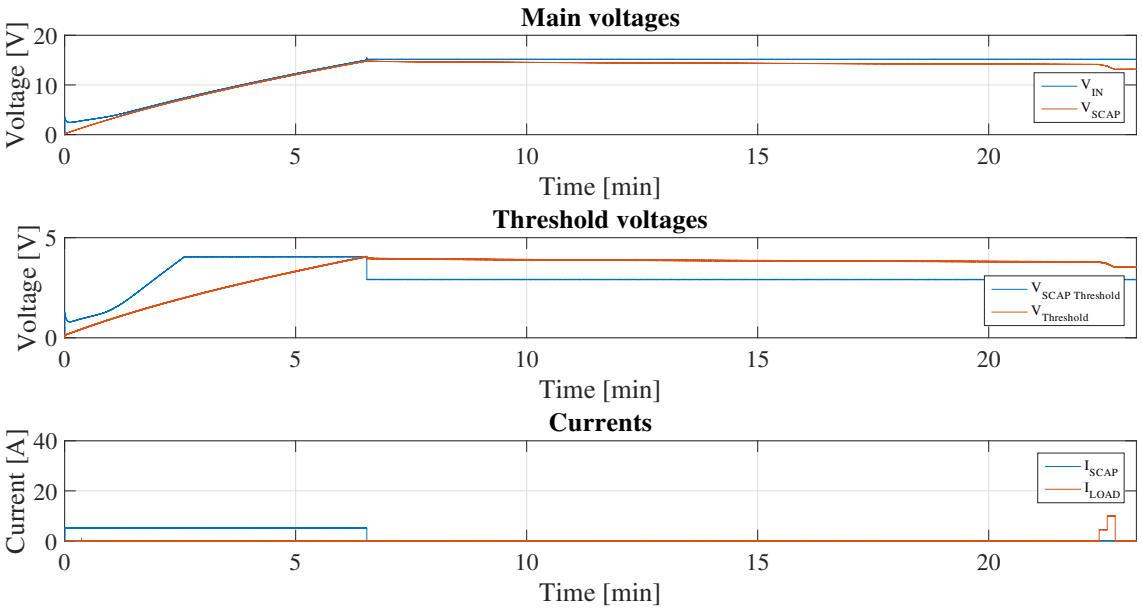

Figure 5.10: Measured voltages and currents for the convenience mode test sequence.

A zoom in of the region where the DC load is applied can be seen in Figure 5.11.

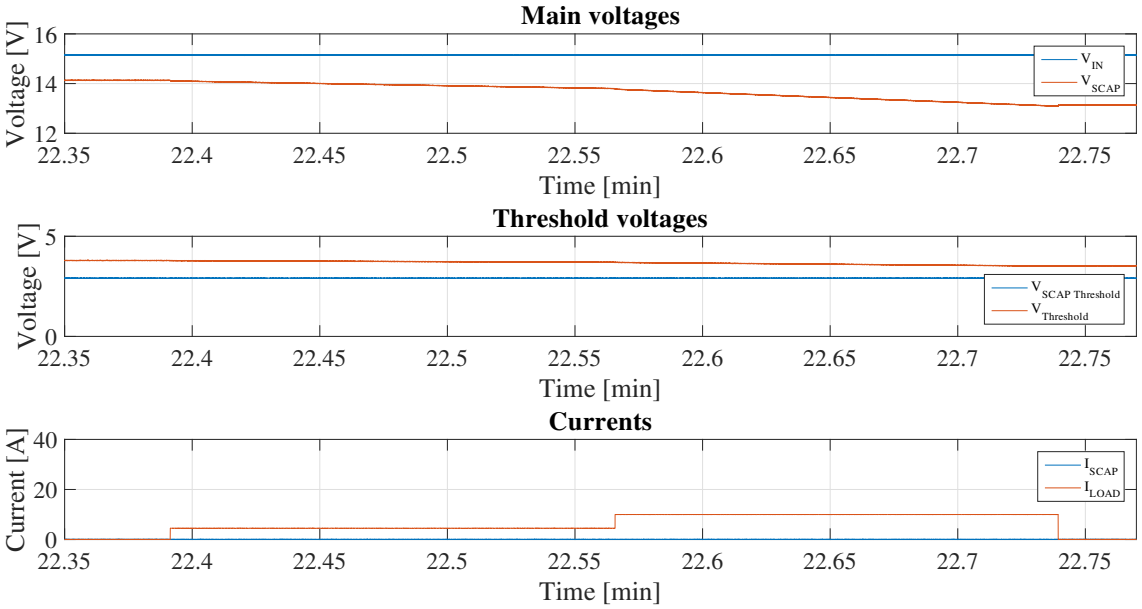

Figure 5.11: Zoom in on the measured time interval where currents increase in the end of the measurement.

5.3.1.4 Test case 4

A summary of the test sequence for 'Test case 4' can be seen in Table 4.3 while the extended explanation is presented in section 4.5.1.4.

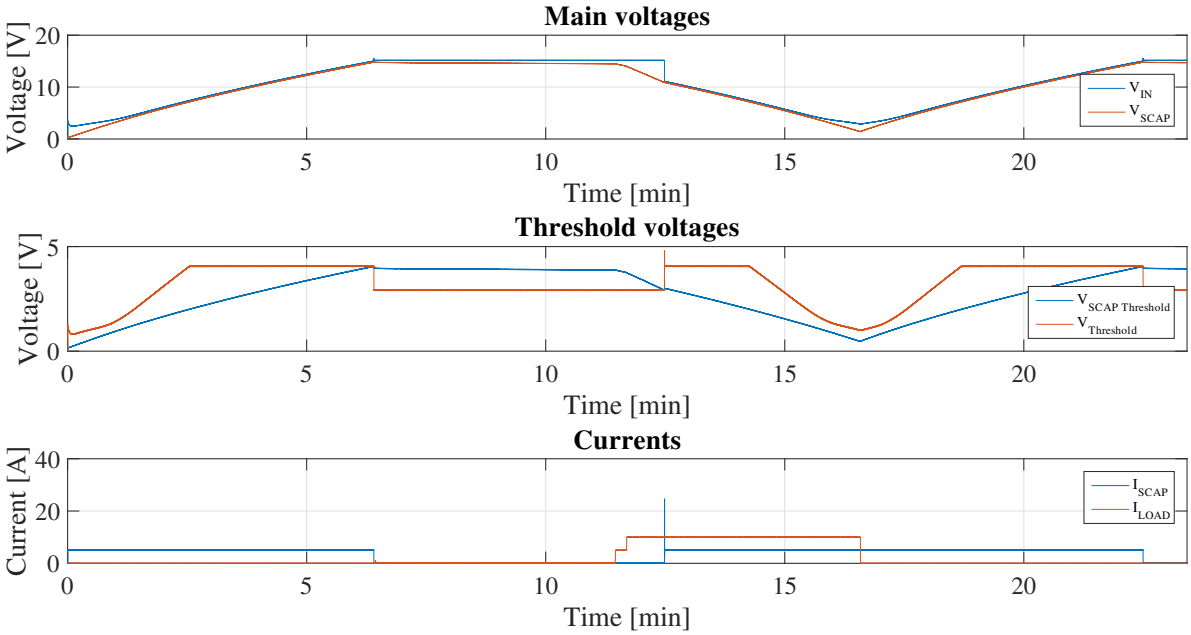

Figure 5.12: Measured voltages and currents for the test case 4 scenario.

5.3.1.5 Test case 5

A summary of the test sequence for 'Test case 5' can be seen in Table 4.3 while the extended explanation is presented in section 4.5.1.5. The test result for the case can be seen in Figure 5.13.

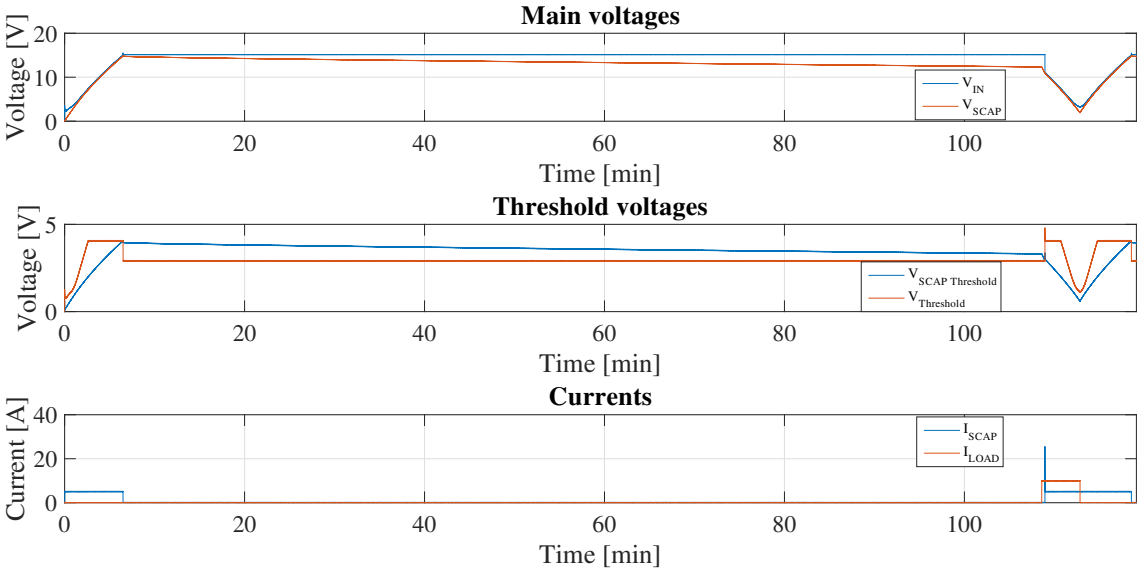

Figure 5.13: Measured voltages and currents for the test case 5 scenario.

A zoom in of the region where the 10A DC load is applied can be seen in Figure 5.14.

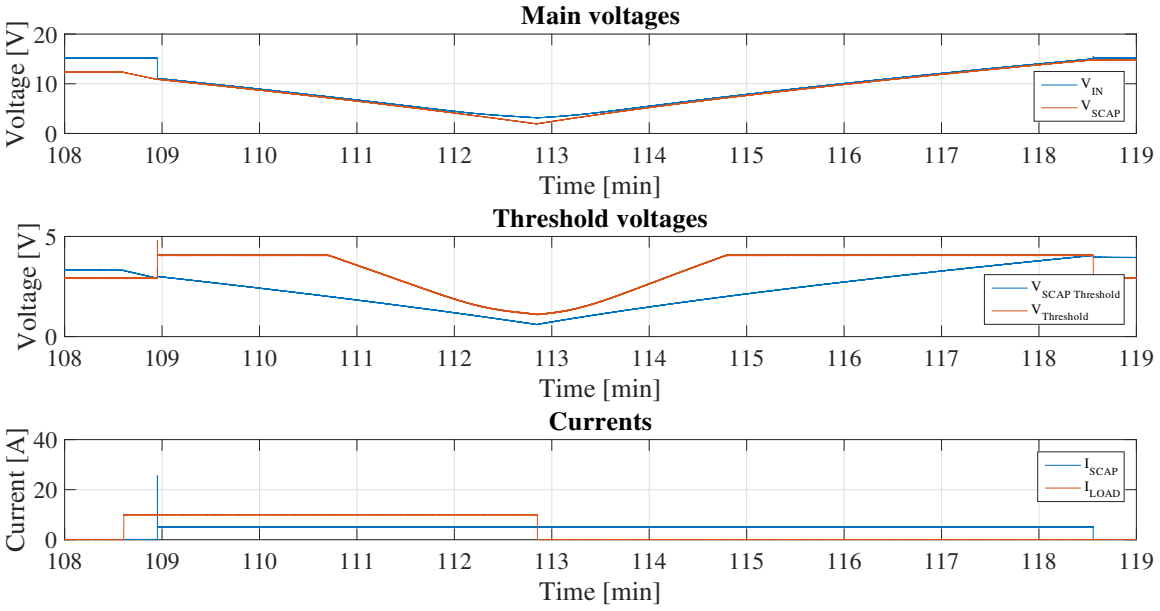

Figure 5.14: Zoom in on the measured voltages and currents for the test case 5 scenario.

5.3.1.6 Test case 6

A summary of the test sequence for 'Test case 6' can be seen in Table 4.3 while the extended explanation is presented in section 4.5.1.6. The test result for the case can be seen in Figure 5.15.

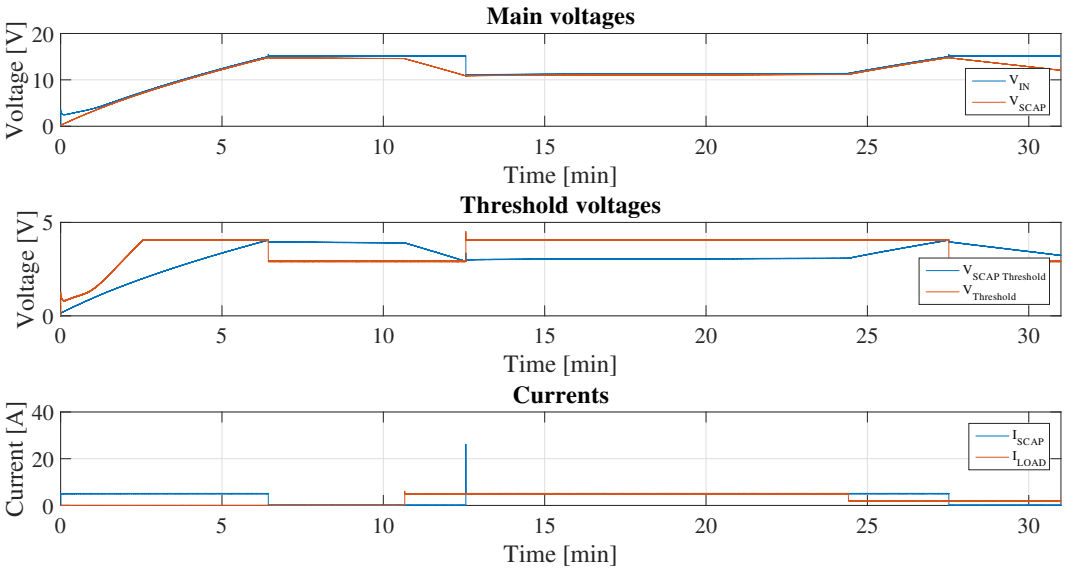

Figure 5.15: Measured voltages and currents for the test case 6 scenario.

5.3.1.7 Test case 7

A summary of the test sequence for 'Test case 7' can be seen in Table 4.3 while the extended explanation is presented in section 4.5.1.7. The test result for the case can be seen in Figure 5.16.

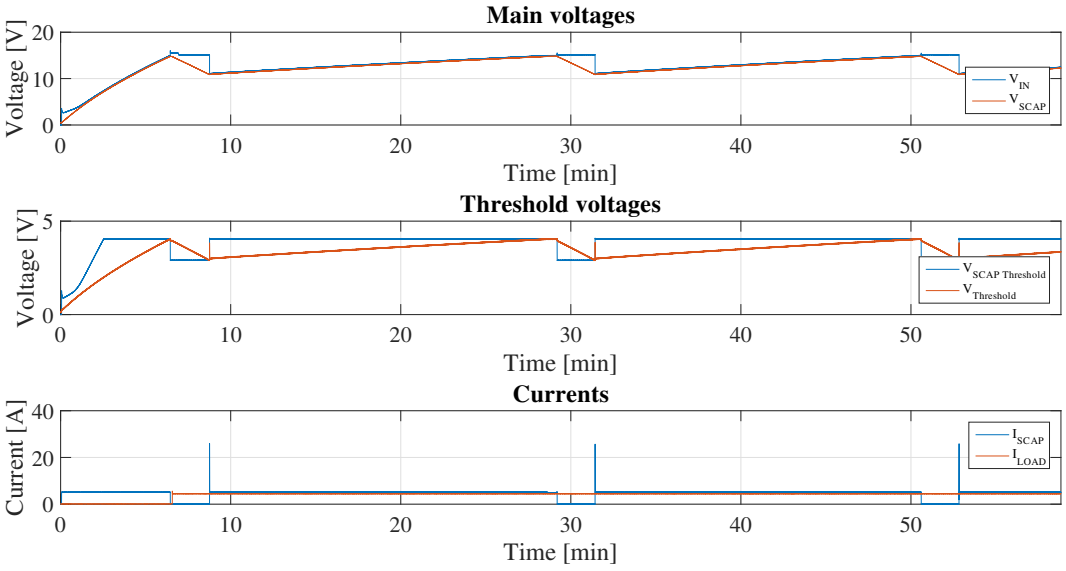

Figure 5.16: Measured voltages and currents for the 'slow charging' test sequence.

5.3.1.8 Inrush current

In all measurements presented it can be seen that as the charging is initiated and the MOSFET transistor is turned on a high inrush current occurs for a very short period of time. This phenomena can be seen in Figure 5.17.

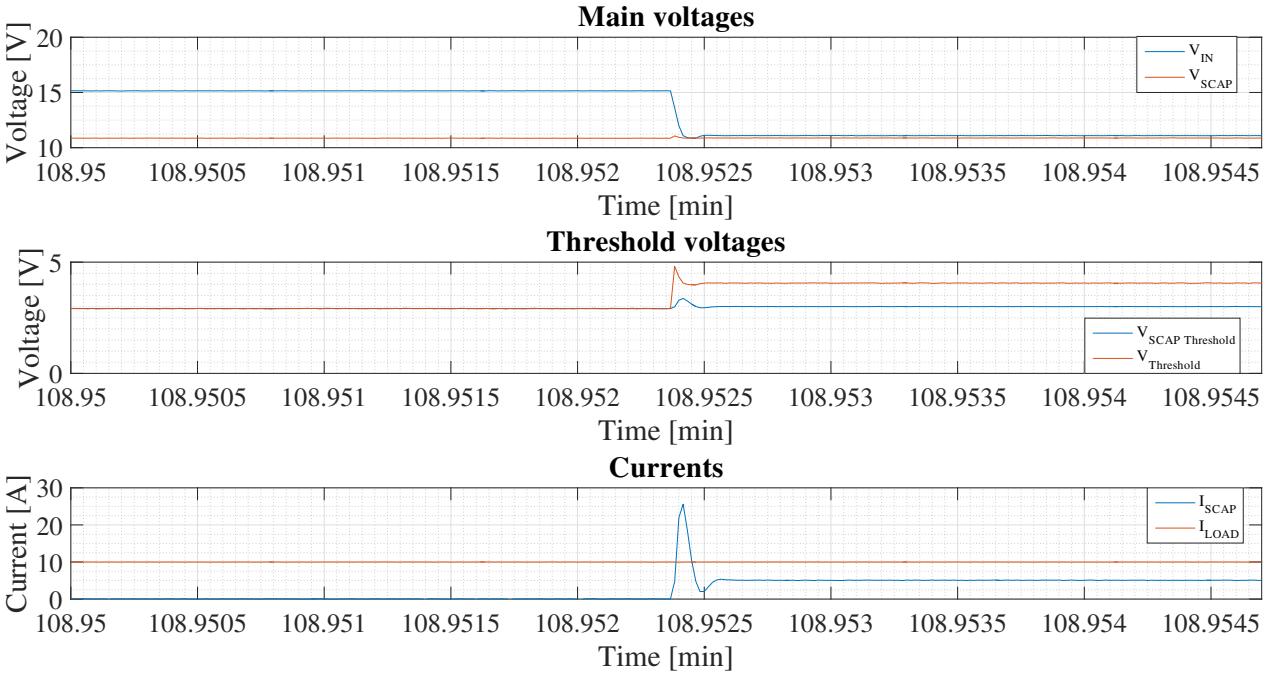

Figure 5.17: Measured inrush current that occurs when MOSFET is switched on.

5.3.2 Measurements in vehicle

Due to the late arrival of the DC/DC converter, there was some time free for alternatives so measurements in a vehicle were performed instead. The tests performed in vehicle with the supercapacitor and comparator circuit were executed according to the test plan in Table 4.3.

5.3.2.1 Abandoned mode

The following was measured when the abandoned mode test sequence was performed in a vehicle according to the test plan in Table 4.3.

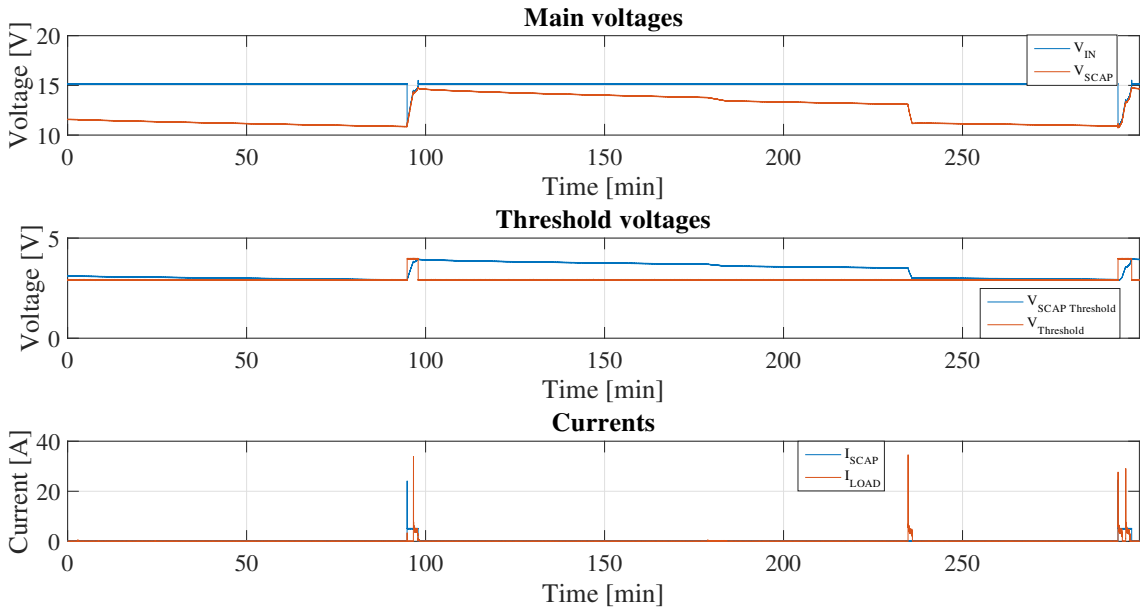

Figure 5.18: Measured voltages and current in vehicle for abandoned mode test sequence.

Where a zoom in of the time period where the voltage level of the supercapacitor reaches $\sim 11V$, and the charging phase is initiated, can be seen Figure 5.19.

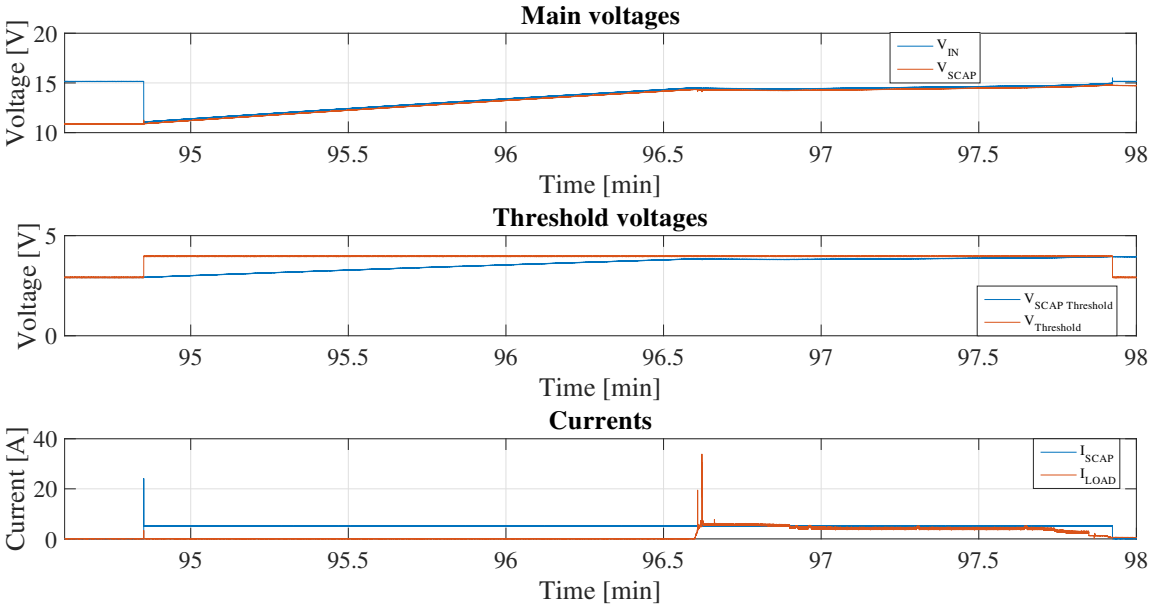

Figure 5.19: Measured voltages and current in vehicle for the zoom in of the charging phase for the abandoned mode test sequence.

5.3.2.2 Inactive mode

The following was measured when the inactive mode test sequence was performed in a vehicle according to the test plan in Table 4.3.

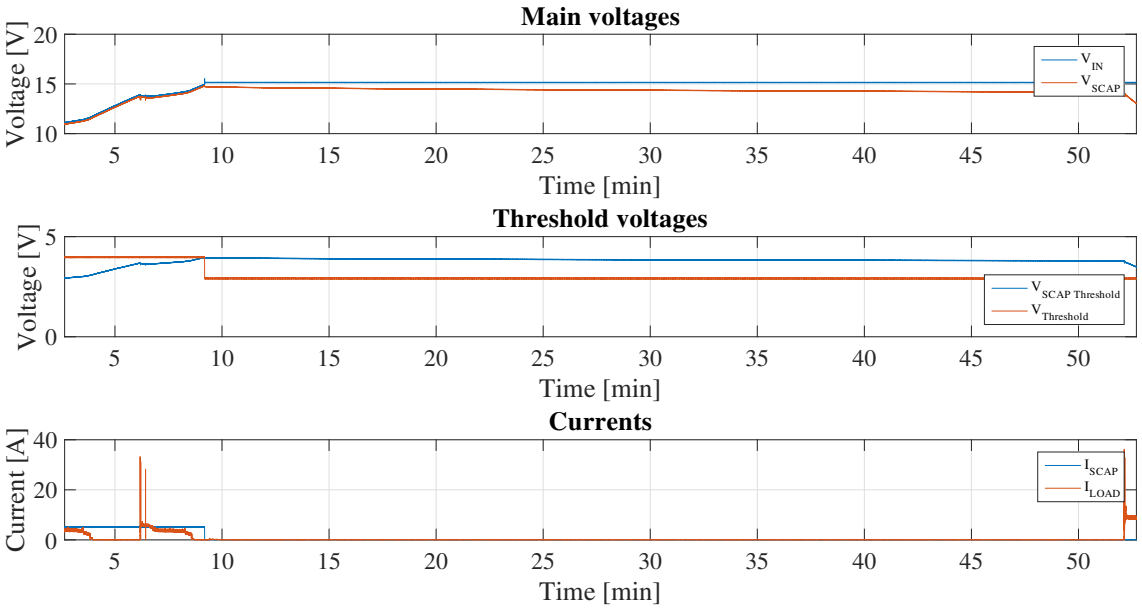

Figure 5.20: Measured voltages and currents in vehicle for inactive mode test sequence.

Where a zoom in of the time period where the vehicle goes from abandoned to inactive, as mentioned in Table 4.3, can be seen Figure 5.21.

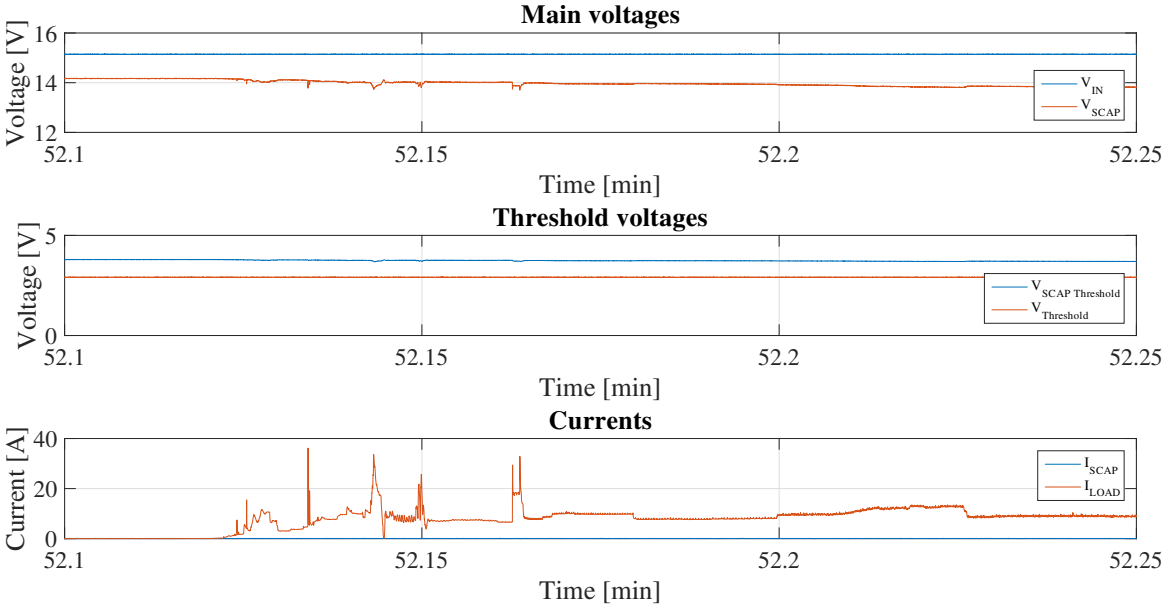

Figure 5.21: Zoom in on measured voltages and currents in vehicle when it goes from abandoned to inactive mode.

5.3.2.3 Convenience mode

The following was measured when the convenience mode test sequence was performed in a vehicle according to the test plan in Table 4.3.

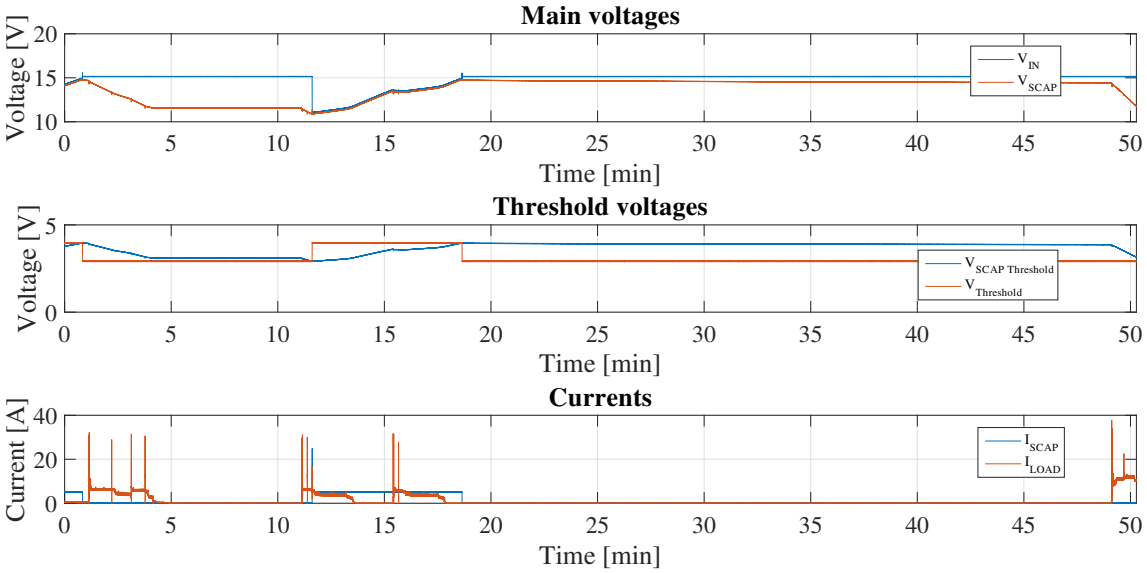

Figure 5.22: Measured voltages and currents in vehicle for inactive mode test sequence.

Where a zoom in of the time period where the vehicle goes from abandoned to inactive and then to convenience can be seen Figure 5.23.

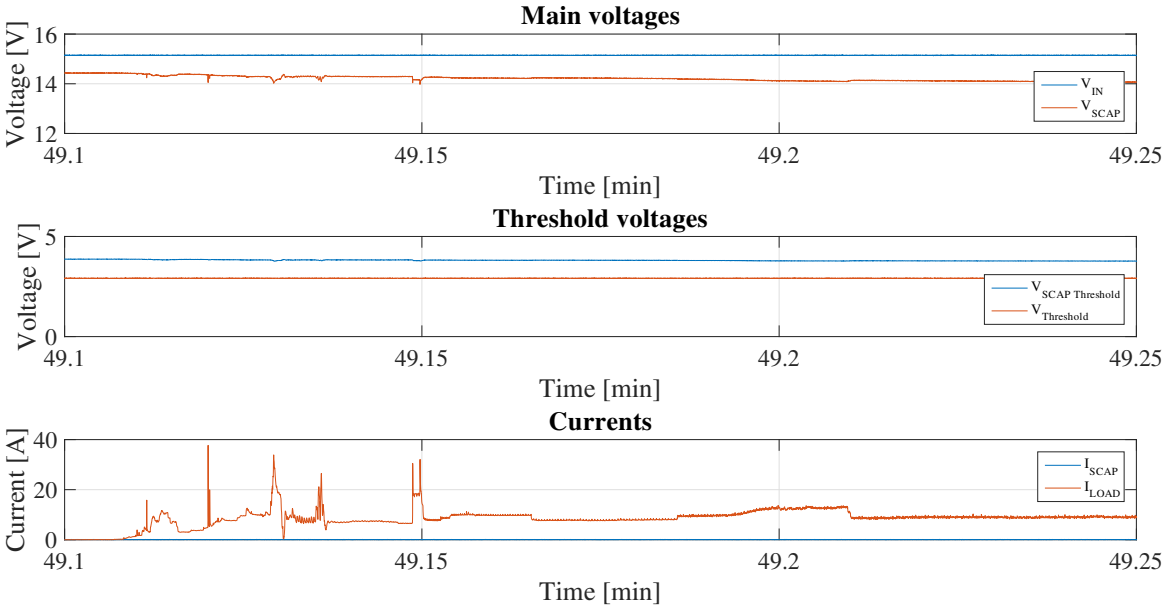

Figure 5.23: Zoom in on measured voltages and currents in vehicle when it goes from abandoned to convenience mode.

5.3.2.4 Active mode

The following was measured when the active mode test sequence was performed in a vehicle according to the test plan in Table 4.3.

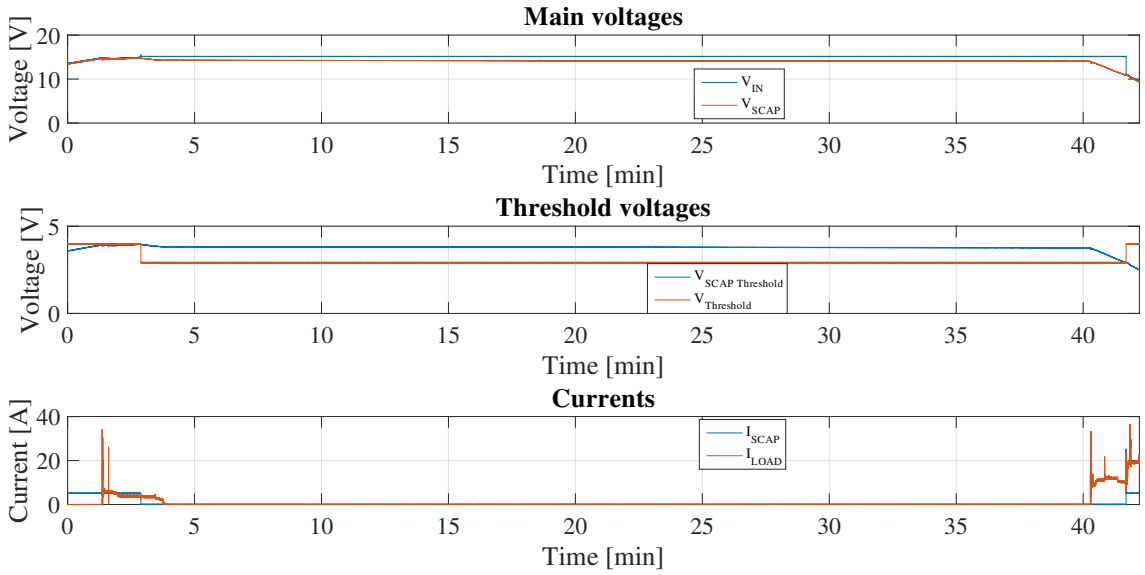

Figure 5.24: Measured voltages and currents in vehicle for active mode test sequence.

Where a zoom in of the time period where the vehicle goes from abandoned to inactive, to convenience and then to active can be seen Figure 5.25.

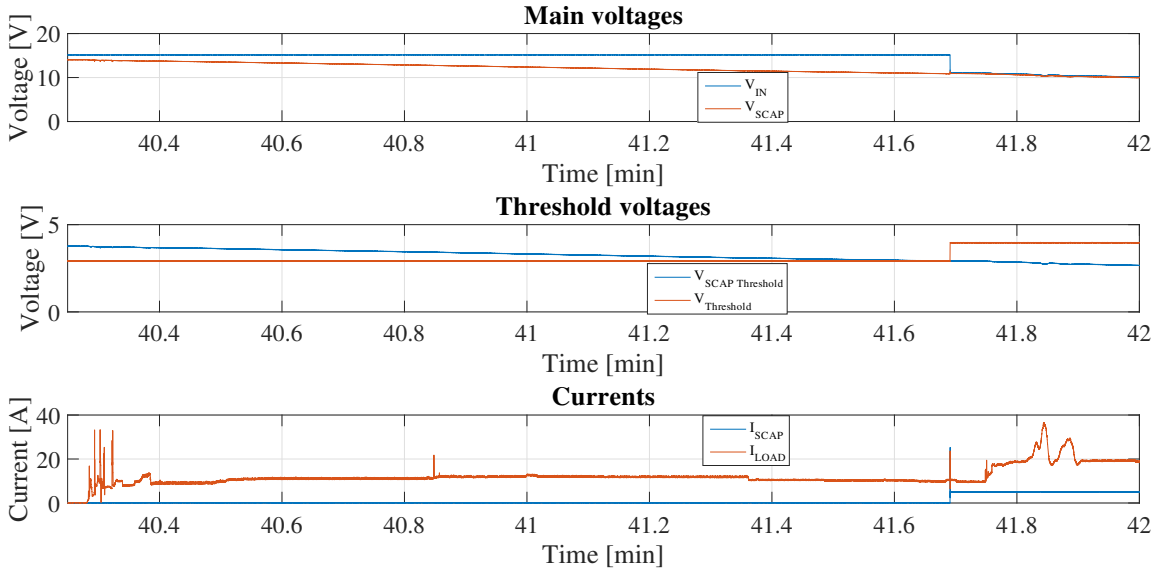

Figure 5.25: Zoom in on measured voltages and currents in vehicle when it goes from abandoned to active mode.

6
Discussion

6.1 Supercapacitor dimensioning and design types

Looking at the supercapacitor, increasing the capacitance would lead to a higher energy storage, but at the expense of increasing volume, weight and cost. Therefore a balance between capacitance and the three has to be made, based on the desired outcome. Based on the capacitance of each capacitor unit, design type a or b presented in the theory section should be used. If the capacitance per unit is 'lower', then the design with two parallel branches should be used in order to 'reach' the desired total capacitance. This design will result in a lower internal resistance based on equation 6.1

$$R_{internal} = \frac{R_1 R_2}{R_1 + R_2}. \tag{6.1}$$

A lower internal resistance enables for a higher peak current based on ohms law

$$I = \frac{U_{supercapacitor}}{R_{internal}} \tag{6.2}$$

along with lower losses due to

$$P = RI^2. \tag{6.3}$$

Having a higher number of separate, smaller capacitors within the supercapacitor module to reach a specific capacitance will increase the size of the module, but will also enable for a higher peak current to be drawn. Therefore, as mentioned previously, it is a balance based on the desired outcome and usage area.
In the current usage mode for the supercapacitor the peak current is highly regarded as it is used to reignite the combustion engine. But in this project the supercapacitor is used to supply the 12V electrical system with energy, therefore a high peak current is not as important as a high capacitance to supply a lower current for a longer time period, hence both design types have their advantages and disadvantages based on the usage mode.

6.2 Circuit design and alternatives

If the concept and thereby the circuit was to be implemented in the future vehicles, some of the components could be replaced by more standardized options with similar functionalities that are cheaper. In this thesis the availability of some components from the supplier was more important than using a standardized option in the industry due to the short time schedule.

6.3 Results

As mentioned in section 4.3.1 the simulations performed to charge the supercapacitor were not executed with the full 'chain' but rather with a customized circuit that forced the supercapacitor to 11V at 5ms and then charged it to 15V. The supercapacitor in the simulations was not the full-size unit but rather a fraction of the total capacitance as the characteristics are identical besides from time intervals. This due to the extremely long simulation times if using the DC/DC step-down converter operating at $100kHz$ and the full $120F$ supercapacitor. But the voltage characteristics charging the smaller capacitance are as expected, with a flattening curve when approaching the rated voltage of 15V.

This concept works very well and handles the various usages modes with the predicted outcomes, where the 'convenience' and 'active' usage modes are problematic if stayed in for too long as it drains the supercapacitor since the circuit cannot provide the 10-20A, but rather 5A. Which means that if the 12V electrical system consumes 15A and the comparator circuit can supply 5A there will be a net loss of 10A from the supercapacitor continuously. The 'active' usage mode is very rarely used by the common customer and since all ECU's are activated it can be discussed whether the large 48V DC/DC converter should be active or not. Therefore the 'active' usage mode shall not be considered when dimensioning the system, but rather the convenience mode.

It can be seen in all test results using the 15V power supply that once the voltage level of the supercapacitor reaches 11V and the MOSFET transistor turns on the charging a short, but high, inrush current of $\sim 25A$ occurs. The time period is approximately $100\mu s$ so it is not dangerous to the circuit, but still an undesired behaviour. This current occurs partly due to the operating frequency of the 15V power supply, which is not high enough to fully control the current output when the charging of the supercapacitor is initiated. In addition, it is partly due to the DC characteristics of a capacitor, which in an ideal case has an infinite resistance in DC, which means that when the MOSFET turns on the inrush current will be higher as the resistance is lower but as time passes the voltage becomes a pure DC and the resistance becomes infinite again. This can be seen in equation 6.4

$$Z = \frac{1}{wC} \tag{6.4}$$

as $w \to 0$, Z will be infinite.

6.4 Life cycles

When analyzing statistics it can be seen that the average vehicle spends approximately $3 - 4\%$ of each day driving and the remaining time being parked, that is approximately 1 hour of driving and 23 hours parked [10]. As can be seen in Table 3.1 the lead-acid batteries have between 500 and 2000 cycles depending on the technology used, compared to the supercapacitor which has approximately 500 000 cycles, as mentioned in 3.3.2. When the vehicle is in abandoned mode most ECU's are asleep, which means that they do not consume any power. So by assuming that the average quiescent current during the 23 hours parked with the vehicle in abandoned mode is

$$I_{averagequiescent} = 15mA$$

and one discharge cycle of the supercapacitor takes

$$T_{discharge} = \frac{C}{I_{averagequiescent}} dU = \frac{120}{0.015} \cdot 4 = 8.88h$$

summed together with a charging time from 11V to 15V of

$$T_{charge} = \frac{120}{5} \cdot 4 = 1.6minutes = 0.0267h$$

equals approximately 8.9 hours per discharge-charge cycle for the supercapacitor. One life cycle equals $15V \rightarrow 0V + 0V \rightarrow 15V$, which corresponds to

$$\frac{\text{one life cycle}}{\text{one discharge-charge cycle}} = \frac{30V}{8V} = 3.75$$

discharge-charge cycles in order to have 'used' one life cycle. The total number of hours parked in a year is

$$\text{hours parked in a year} = 23 \cdot 365.24 = 8400.5.$$

which then results in

$$\text{life cycles per year} = \frac{8400.5}{8.9 \cdot 3.75} = 251.7.$$

The comparison can be seen in Table 6.1.

Table 6.1: Life cycles per year and in total for both lead-acid batteries and supercapacitor.

Type	Technology	Quiescent current	Life cycles per year	Life cycles total	Usage time (in years)
Battery	Flooded	15mA	125	500	4
	AGM		500	2000	
Supercapacitor	-	15mA	251.7	500 000	1986.5

It can be concluded that the supercapacitor due to its large number of life cycles is exceptional when it comes to low power cycling like the 'Abandoned' usage mode in vehicles. But it also has to be noted that the usage time is a theoretical value and the real life usage time will be way lower due to exposure to temperature, vibrations and electrical events.

6.5 Future work

The operational amplifiers in the comparator circuit in this project have been used to control the switching of a MOSFET transistor based on the voltage level over the supercapacitor. An interesting alternative to the MOSFET would be to have the operational amplifiers instead control the DC/DC step-down converter by connecting the output of the OP-AMP (CompOut) to the SHDN pin on the LT3845 DC/DC converter. By doing this one object in the 'chain' is removed, which could result in lower losses and less components. The proposed layout of the alternative described can be seen in Figure 6.1.

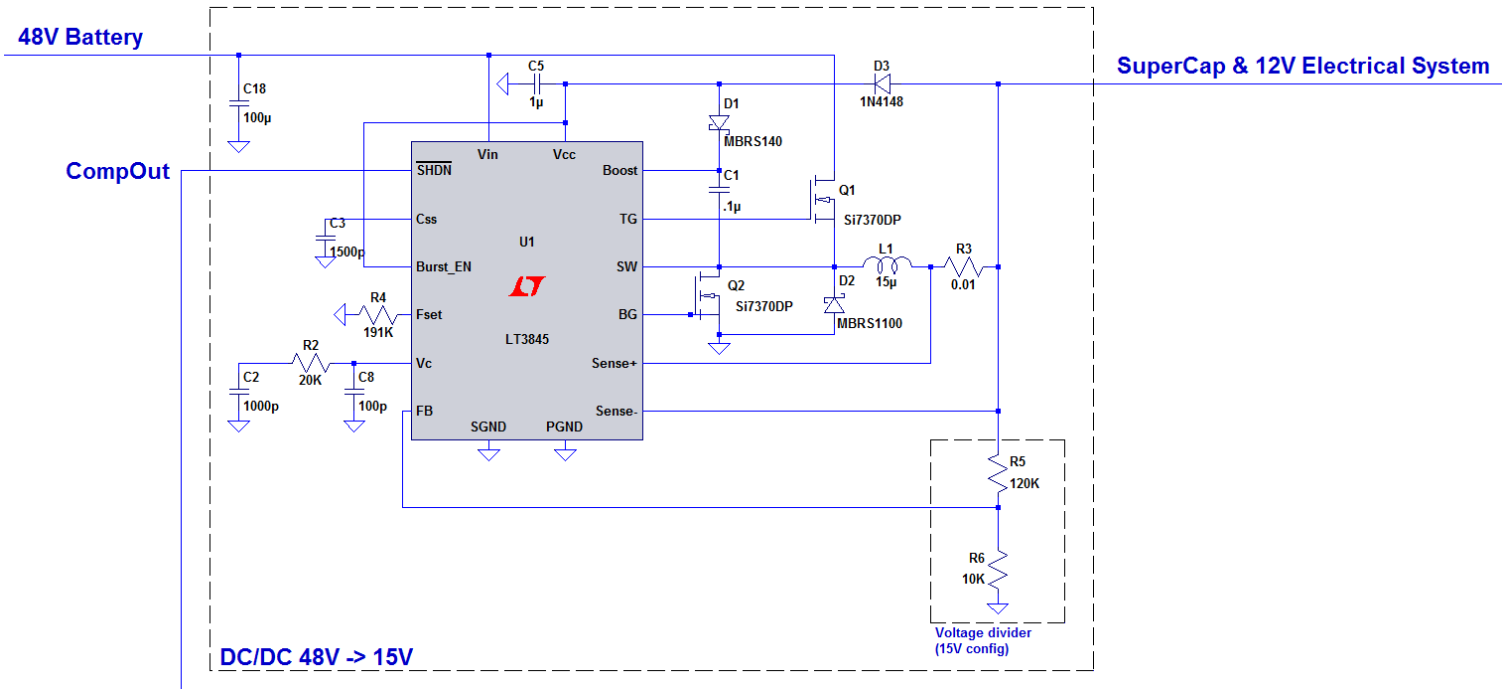

Figure 6.1: Circuit layout for the proposed future work.

If the solution was to be implemented in a vehicle and thereby replace the 12V lead-acid battery while fulfilling all requirements on the 12V lead-acid battery, a small support-battery is necessary. Since the batteries have the ability to support the vehicle with power for a longer time period, as for example during a generator failure, which is when the generator is not charging when it should. The supercapacitor alone cannot supply the vehicle with for example 50A for two minutes, but together with a support battery it could be achieved. One of the advantages of using a supercapacitor instead of a battery is the amounts of life cycles the supercapacitor

has compared to the battery. Therefore, if a support battery is connected in parallel with the supercapacitor, the recommended lower voltage threshold would be above the nominal voltage of the support battery. In order to avoid cycling the battery when the vehicle is in Abandoned, Inactive or Convenience modes.

6.6 Recommendation

The results indicate that the concept works as desired, hence the battery functions are fulfilled. Combined with the calculations regarding life cycles this should be considered a viable alternative to the current lead-acid battery solution. If combined with a support battery all functions mentioned in the Scope would be fulfilled since the support battery has the electrical characteristics of the larger 12V lead-acid batteries but is much smaller, since it will only be supporting in failure situations. A support battery has dimensions 150x85x130 (LxWxH) mm and the supercapacitor, as mentioned in section 3.3.2, 120x130x80 (LxWxH) mm. This results in a combined volume of $V_{SCap+SupBatt} = 2944.5cm^3$, and if not possible to slot in next to each other it can be approximated to $V_{SCap+SupBatt} = 3000cm^3$. In terms of weight the supercapacitor module with the PCB circuit encapsulated weighs approximately 1.6kg and the support battery 4.4 kg. Comparison of the two alternatives can be seen in Table 6.2.

Table 6.2: Comparison between current and optional solutions (Lifetime for supercap is a theoretical value).

Alternative	Volume (cm^3)	Weight (kg)	Life time (years)
12V Lead-acid battery	10395	21	3-4
SuperCap + Support Battery	3000	6	Vehicles life time

Therefore the concept is recommended and hopefully development will push it further and eventually integrate it into mass-produced vehicles.

7
Ethical aspects

The lead-acid batteries are used in all parts of the world in various different industries besides from the automotive industry. Approximately all main and support batteries in the automotive industry on 12V are of lead-acid type, which makes this project very relevant as replacing the battery with a less harmful solution to both nature and the human body is of great interest [1]. Lead-acid batteries that are being recycled are opened up and the materials within are separated in order for the materials to be re-used. In some countries this process is executed by children, who are extremely susceptible to lead and will be affected in the long term as their body is growing and the lead attacks the organs and disrupt their development. This can, amongst several conditions, result in abnormal brain functionality, nervous system disorder or serious kidney damage [2].

As the automotive industry is selling several million vehicles per year, the lead in the conventional 12V battery cannot solely originate from recycled batteries but also from mining of new lead. The mining industry and its surrounding activities are some of the largest environmental pollution sources as they release several highly toxic materials into the nature during mining, smelting and transporting. As the heavy metal pollutes the water, soil and air it greatly affects the health of the locals living in the area [3].

Therefore, finding a substitute or alternative to the lead-acid battery is of great importance as it will decrease the need for a material that is highly toxic and affects environment, animals and humans. It will also help in reaching the emission regulations that are set by different global organizations.

8

Conclusion

The theoretical calculations of the charging and discharging times are corresponding to the real times in the tests, which indicates that the power electronics circuit is properly designed. Some deviation is to be expected as the real world diverge from the theoretical world in terms of conduction and power losses.

This project has developed a proof of concept solution that could work as a substitute to the 12V lead-acid battery within the automotive industry. The concept circuit only charges the supercapacitor with a current of 5A, but when the concept is implemented into the automotive industry it should deliver a higher current in order for it to be able to fully replace the 12V lead-acid battery. Mostly since the 'convenience' usage mode consumes approximately 10A and the concept solution only supplies 5A, this means that when the supercapacitor discharges below a certain voltage level some functionalities would stop working as the supplied current and voltage is insufficient.

The supercapacitor + support battery option has both a volume and weight of approximately 30% of the current 12V lead-acid battery option. Due to its lower volume, the concept solution could be positioned in another space within the vehicle, eventually closer to the front of the vehicle where most of the high power loads are positioned. That would reduce weight and cost of the cables, along with lower voltage drops over the cables as they are shorter.

As the automotive industry is rapidly advancing in terms of functionality, an increased number of ECU's fulfilling these functions are implemented into the vehicle. This will lead to an increased average current consumption in the different vehicle modes; abandoned, inactive, convenience and active. When the average current consumption increases, the 12V lead-acid battery is cycled harder, which means that the lifespan is shortened from the already short 2-4 years. Therefore the supercapacitor concept is extremely interesting as the supercapacitor has approximately 500 000 cycles compared to the 500-2000 of a battery, depending on the technology. The electrical architectures where the concept can be used are the 400V and 48V hybrid architectures, where there is a large energy source on the high voltage side that can supply the supercapacitor with energy, which will keep the 12V electrical system running.

Bibliography

[1] Haefliger, P., Mathieu-Nolf, M., Lociciro, S., Ndiaye, C., Coly, M., & Diouf, A. et al. (2009). Mass Lead Intoxication from Informal Used Lead-Acid Battery Recycling in Dakar, Senegal. Environmental Health Perspectives, 117(10), 1535-1540. doi:10.1289/ehp.0900696

[2] van der Kuijp, T., Huang, L., & Cherry, C. (2013). Health hazards of China's lead-acid battery industry: a review of its market drivers, production processes, and health impacts. Environmental Health, 12(1). doi:10.1186/1476-069x-12-61

[3] Zhang, X., Yang, L., Li, Y., Li, H., Wang, W., & Ye, B. (2011). Impacts of lead/zinc mining and smelting on the environment and human health in China. Environmental Monitoring And Assessment, 184(4), 2261-2273. doi:10.1007/s10661-011-2115-6

[4] Barkhordarian, Vrej. "Power MOSFET basics." Powerconversion and Intelligent Motion-English Edition 22.6 (1996).

[5] Ti.com. (2018). [online] Available at: http://www.ti.com/lit/ds/symlink/lm317a.pdf [Accessed 19 Sep. 2018].

[6] Transistors: Types, Materials and Applications, edited by Benjamin M. Fitzgerald, Nova Science Publishers, Incorporated, 2010. ProQuest Ebook Central, https://ebookcentral.proquest.com/lib/chalmers/detail.action?docID=3018159.

[7] Supercapacitors : Materials, Systems and Applications, edited by Francois Beguin, and Elzbieta Frackowiak, John Wiley Sons, Incorporated, 2013. ProQuest Ebook Central, https://ebookcentral.proquest.com/lib/chalmers/detail.action?docID=1166317.

[8] China-Euro Vehicle Technology AB.

[9] Maxwell.com. (2018). [online] Available at: http://www.maxwell.com/images/documents/K2Series$_D$S$_1$015370$_{52}$0141104.*pdf*[*Accessed*22*Oct*

[10] Racfoundation.org. (2018). [online] Available at: https://www.racfoundation.org/assets/rac$_f$*oundation*/*content*/*downloadables*/*spaced*$_o$*ut*−*bates*$_l$*eibling* − *jul*12.*pdf*[*Accessed*22*Oct*.2018].

A

Appendix 1

Ref. Name	Value	Manufacturer	Manufacturer part no.	Vendor	Vendor component nr.	Quantity	Unit price ($)	Price ($)
A		Texas Instruments	TLV6002IDR	Digikey	296-47357-1-ND	2	0,78	1,56
B		Texas Instruments	TLV6002IDR	Digikey	296-47357-1-ND	2	0,78	1,56
C1	100u	Nichicon	UVY1E101MDD1TD	Digikey	493-12902-1-ND	2	0,31	0,62
C2	100u	Nichicon	UVY1E101MDD1TD	Digikey	493-12902-1-ND	2	0,31	0,62
C3	1u	KEMET	C1206C105K3RACTU	Digikey	399-1255-1-ND	2	0,32	0,64
C4	0,1u	KEMET	C1206F104K3RACTU	Digikey	399-5615-1-ND	2	0,46	0,92
C5	1u	KEMET	C1206C105K3RACTU	Digikey	399-1255-1-ND	2	0,32	0,64
C6	0,1u	KEMET	C1206F104K3RACTU	Digikey	399-5615-1-ND	2	0,46	0,92
C7	0,1u	KEMET	C1206F104K3RACTU	Digikey	399-5615-1-ND	2	0,46	0,92
C8	0,1u	KEMET	C1206F104K3RACTU	Digikey	399-5615-1-ND	2	0,46	0,92
C9	0,1u	KEMET	C1206F104K3RACTU	Digikey	399-5615-1-ND	2	0,46	0,92
C10	0,1u	KEMET	C1206F104K3RACTU	Digikey	399-5615-1-ND	2	0,46	0,92
C11	0,1u	KEMET	C1206F104K3RACTU	Digikey	399-5615-1-ND	2	0,46	0,92
C12	100u	Nichicon	UVY1E101MDD1TD	Digikey	493-12902-1-ND	2	0,31	0,62
D1		ON Semiconductor	MMBZ33VALT1G	Digikey	MMBZ33VALT1GOSCT-ND	2	0,21	0,42
D2		Micro Commercial Co	1N4148W-TP	Digikey	1N4148WTPMSCT-ND	2	0,14	0,28
D3		Micro Commercial Co	1N4148W-TP	Digikey	1N4148WTPMSCT-ND	2	0,14	0,28
D4		OSRAM Opto Semiconductors Inc.	LH R974-LP-1	Digikey	475-1415-1-ND	2	0,36	0,72
D5		OSRAM Opto Semiconductors Inc.	LG R971-KN-1	Digikey	475-1410-1-ND	2	0,36	0,72
D6		Micro Commercial Co	1N4148W-TP	Digikey	1N4148WTPMSCT-ND	2	0,14	0,28
D7		OSRAM Opto Semiconductors Inc.	LG R971-KN-1	Digikey	475-1410-1-ND	2	0,36	0,72
D8		OSRAM Opto Semiconductors Inc.	LG R971-KN-1	Digikey	475-1410-1-ND	2	0,36	0,72
J1		Phoenix Contact	1935161	Digikey	277-1667-ND	2	0,41	0,82
J2		Phoenix Contact	1935161	Digikey	277-1667-ND	2	0,41	0,82
LM317A		Texas Instruments	LM317AEMPX/NOPB	Digikey	LM317AEMPX/NOPBCT-ND	2	1,74	3,48
Q1		Micro Commercial Co	MCQ4435-TP	Digikey	MCQ4435-TPMSCT-ND	2	0,62	1,24
Q2		Micro Commercial Co	MMSS8050-H-TP	Digikey	MMSS8050-H-TPMSCT-ND	2	0,21	0,42
Q3		Micro Commercial Co	MMSS8050-H-TP	Digikey	MMSS8050-H-TPMSCT-ND	2	0,21	0,42
Q4		Micro Commercial Co	MMSS8050-H-TP	Digikey	MMSS8050-H-TPMSCT-ND	2	0,21	0,42
Q5		Micro Commercial Co	MMSS8050-H-TP	Digikey	MMSS8050-H-TPMSCT-ND	2	0,21	0,42
R1	270	Yageo	RC1206FR-07270RL	Digikey	311-270FRCT-ND	2	0,1	0,2
R2	10m	Yageo	RL1206FR-7W0R01L	Digikey	311-.01LYCT-ND	2	0,73	1,46

R3	820	Yageo	RC1206JR-07820RL	Digikey	311-820ERCT-ND	2	0,1	0,2
R4	5K	Yageo	RT1206BRD075KL	Digikey	YAG5090CT-ND	2	0,58	1,16
R5	1K	Yageo	RC1206JR-071KL	Digikey	311-1.0KERCT-ND	2	0,1	0,2
R6	1K	Yageo	RC1206JR-071KL	Digikey	311-1.0KERCT-ND	2	0,1	0,2
R7	100K	Yageo	RT1206DRD07100KL	Digikey	311-2914-1-ND	2	0,35	0,7
R8	9.1K	Yageo	RC1206JR-079K1L	Digikey	311-9.1KERCT-ND	2	0,1	0,2
R9	1K	Yageo	RC1206JR-071KL	Digikey	311-1.0KERCT-ND	2	0,1	0,2
R10	1K	Yageo	RC1206JR-071KL	Digikey	311-1.0KERCT-ND	2	0,1	0,2
R11	8,06K	Panasonic Electronic Components	ERA-8AEB8061V	Digikey	P8.06KBCCT-ND	2	0,1	0,2
R12	2,49K	Yageo	RC1206FR-072K49L	Digikey	311-2.49KFRCT-ND	2	0,1	0,2
R13	22K	Yageo	RC1206JR-0722KL	Digikey	311-22KERCT-ND	2	0,1	0,2
R14	10K	Yageo	RT1206FRE0710KL	Digikey	YAG1242CT-ND	2	0,15	0,3
R15	100K	Yageo	RT1206DRD07100KL	Digikey	311-2914-1-ND	2	0,35	0,7
R16	100K	Yageo	RT1206DRD07100KL	Digikey	311-2914-1-ND	2	0,35	0,7
R17	100K	Yageo	RT1206DRD07100KL	Digikey	311-2914-1-ND	2	0,35	0,7
R18	100K	Yageo	RT1206DRD07100KL	Digikey	311-2914-1-ND	2	0,35	0,7
R19	100K	Yageo	RT1206DRD07100KL	Digikey	311-2914-1-ND	2	0,35	0,7
R20	100K	Yageo	RT1206DRD07100KL	Digikey	311-2914-1-ND	2	0,35	0,7
R21-R3	-	-	-	-	-	-	-	-
R24	20K	Bourns Inc.	3306F-1-203	Digikey	3306F-203-ND	2	0,43	0,86
R25	1K	Yageo	RC1206JR-071KL	Digikey	311-1.0KERCT-ND	2	0,1	0,2
R26	10m	Yageo	RL1206FR-7W0R01L	Digikey	311-.01LYCT-ND	2	0,73	1,46
R27	470	Yageo	AC1206FR-07470RL	Digikey	YAG3879CT-ND	2	0,1	0,2
R28	1K	Yageo	RC1206JR-071KL	Digikey	311-1.0KERCT-ND	2	0,1	0,2
R29	510	Yageo	AC1206FR-07510RL	Digikey	YAG3887CT-ND	2	0,1	0,2
R30	10K	Bourns Inc.	3306P-1-103	Digikey	3306P-103-ND	2	0,43	0,86
R31	20K	Bourns Inc.	3306F-1-203	Digikey	3306F-203-ND	2	0,43	0,86
R32	510	Yageo	AC1206FR-07510RL	Digikey	YAG3887CT-ND	2	0,1	0,2
R33	120	Yageo	RC1206JR-07120RL	Digikey	311-120ERCT-ND	2	0,1	0,2
DC/DC Conv		Analog Devices	DC1073A	Mouser	584-DC1073A	1	132,6	132,6
Standoffs		Harwin Inc.	R30-9401400	Digikey	952-3020-ND	4	0,3	1,2
						Total:	173,74	

Comment	Datasheet
OP-AMP	http://www.ti.com/lit/ds/symlink/tlv6001.pdf
OP-AMP	http://www.ti.com/lit/ds/symlink/tlv6001.pdf
Through-hole mounted	
Through-hole mounted	
Through-hole mounted	
MOSFET protection	http://www.onsemi.com/pub/Collateral/MMBZ5V6ALT1-D.PDF
	http://www.mccsemi.com/up_pdf/1N4148W(SOD123).pdf
	http://www.mccsemi.com/up_pdf/1N4148W(SOD123).pdf
LED diode (R)	https://dammedia.osram.info/media/resource/hires/osram-dam-2493888/LH%20R974.pdf
LED diode (G)	https://dammedia.osram.info/media/resource/hires/osram-dam-2493936/LG%20R971.pdf
	http://www.mccsemi.com/up_pdf/1N4148W(SOD123).pdf
LED diode (G)	https://dammedia.osram.info/media/resource/hires/osram-dam-2493936/LG%20R971.pdf
LED diode (G)	https://dammedia.osram.info/media/resource/hires/osram-dam-2493936/LG%20R971.pdf
	https://media.digikey.com/pdf/Data%20Sheets/Phoenix%20Contact%20PDFs/1935161.pdf
	https://media.digikey.com/pdf/Data%20Sheets/Phoenix%20Contact%20PDFs/1935161.pdf
	http://www.ti.com/lit/ds/symlink/lm317a.pdf
MOSFET	http://www.mccsemi.com/up_pdf/MCQ4435(SOP-8)-B.pdf
NPN	http://www.mccsemi.com/up_pdf/MMSS8050(SOT-23).pdf
NPN	http://www.mccsemi.com/up_pdf/MMSS8050(SOT-23).pdf
NPN	http://www.mccsemi.com/up_pdf/MMSS8050(SOT-23).pdf
NPN	http://www.mccsemi.com/up_pdf/MMSS8050(SOT-23).pdf

N/A	
Potentiometer	https://www.bourns.com/docs/Product-Datasheets/3306.pdf
Potentiometer	https://www.bourns.com/docs/Product-Datasheets/3306.pdf
Potentiometer	https://www.bourns.com/docs/Product-Datasheets/3306.pdf
DC/DC Step-down converter evaluation board	